



A new species of brilliant green frog of the genus *Tlalocohyla* (Anura, Hylidae) hiding between two volcanoes of northern Costa Rica

DONALD VARELA-SOTO¹, JUAN G. ABARCA^{2,3*}, ESTEBAN BRENES-MORA^{3,4}, VALERIA ASPINALL³, TWAN LEENDERS⁵ & ALEX SHEPACK⁶

¹Tapir Valley Nature Reserve, Bijagua, Upala, Costa Rica.

✉ donaldivscr@gmail.com; <https://orcid.org/0000-0002-1926-0828>

²Laboratorio de Recursos Naturales y Vida Silvestre, Escuela de Ciencias Biológicas, Universidad Nacional, Heredia, Costa Rica.

✉ barcazajuan@gmail.com; <https://orcid.org/0000-0002-1261-4400>

³Costa Rica Wildlife Foundation, San José, Costa Rica.

✉ valeriaspinall97@gmail.com; <https://orcid.org/0000-0003-4032-8978>

⁴Re:Wild, PO Box 129, Austin, Texas 78767, USA.

✉ ebrenes@rewild.org; <https://orcid.org/0000-0003-2906-8546>

⁵Division of Vertebrate Zoology, Yale Peabody Museum of Natural History, 170 Whitney Avenue, New Haven, CT, 06520, USA.

✉ twanleenders@scinax.com; <https://orcid.org/0000-0003-4166-5001>

⁶Department of Biological Sciences, University of Notre Dame, South Bend, IN 46556, USA.

✉ ashepack@nd.edu; <https://orcid.org/0000-0003-0623-0969>

*Corresponding author. ✉ barcazajuan@gmail.com

Abstract

A new species of hylid frog is described from Tapir Valley Nature Reserve, located on the Caribbean slope of Tenorio Volcano in Bijagua, Alajuela Province, Costa Rica. A molecular phylogenetic analysis supports its inclusion in the genus *Tlalocohyla*. Morphological, morphometric, larval, and acoustic characteristics further distinguish it from other species in the genus and support its uniqueness. The new species is closely related to *T. picta* and *T. smithii*, and is separated by at least 500 kilometers from the nearest known occurrence of a population of *T. picta* in southern Honduras. The new species is readily distinguished from all other *Tlalocohyla* by its brilliant green coloration marked with a pronounced, incomplete light dorsolateral stripe that is bordered above by a diffuse reddish-brown stripe. Its dorsum is marked with bold reddish brown spots and its ventral skin is fully transparent. This new *Tlalocohyla* is currently only known from the type locality, where it inhabits a lentic wetland system with an emergent herbaceous vegetation-dominated benthic zone, surrounded by tropical rainforest. A description of its bioacoustic repertoire and information on natural history, reproduction and habitat preference of this new species are provided.

Key words: *Tlalocohyla celeste* sp. nov., Amphibia, Middle America, Costa Rica, Hylidae, tree frog, taxonomy, endangered species

Resumen

Se describe una nueva especie de rana arborícola de la Reserva Natural Valle del Tapir en Bijagua de Alajuela, localizada en las faldas del Volcán Tenorio en el Caribe norte de Costa Rica. Un análisis filogenético molecular apoya su inclusión en el género *Tlalocohyla*. Características morfológicas, morfométricas, larvarias y acústicas la distinguen de otras especies del género y respaldan su singularidad. La nueva especie está estrechamente relacionada con *T. picta* y *T. smithii*, y está separada por al menos 500 kilómetros lineales de la población conocida más cercana de la primera, en el sur de Honduras. La nueva especie se distingue fácilmente de todos los congéneres por su coloración verde brillante marcada con una franja dorsolateral clara incompleta que está bordeada arriba por una franja difusa de color marrón rojizo. El dorso está marcado con llamativas manchas de color marrón rojizo y su piel ventral es completamente transparente. La nueva especie actualmente solo se conoce de la localidad tipo, en donde habita un sistema de humedales lénticos con una zona béntica dominada por vegetación herbácea emergente, rodeada de bosque tropical. Se proporciona una descripción de su repertorio acústico e información sobre la historia natural, reproducción y preferencia de hábitat de esta nueva especie.

Palabras Claves: *Tlalocohyla celeste* sp. nov., Amphibia, Mesoamérica, Costa Rica, Hylidae, rana arborícola, taxonomía, especies en peligro.

Introduction

Hylidae (Rafinesque 1815) represents the world's largest family of anurans and concomitantly, Hylinae (Rafinesque 1815), is the most speciose within the clade and most of its members are found in the Americas (Faivovich et al. 2005; Frost 2022). Faivovich *et al.* (2005) completely revised the subfamily Hylinae, reviewed the evidential basis of the existing taxonomy, and erected or resurrected several genera based on their hypothesized relationships. The genus *Tlalocohyla* (Faivovich *et al.* 2005) contains four species that were previously included in the *Hyla picta* and *H. godmani* groups as defined by Duellman (1970), but which were later transferred into the *H. godmani* species group by Duellman (2001) based on skull morphology, axillary membrane, and chromosome number. To date, the four species contained in this genus are grouped together based on molecular synapomorphies but without any readily discernible morphological synapomorphy (Faivovich *et al.* 2005). As currently understood, the monophyly of the clade composed by *T. godmani* (Günther 1901) and *T. loquax* (Gaige & Stuart 1934) is well supported, but the relationships of *T. picta* (Günther 1901) and *T. smithii* (Boulenger 1902) remains poorly supported (Faivovich *et al.* 2018). The distribution of the genus *Tlalocohyla* is restricted to Middle America and reaches its greatest diversity in southern Mexico; only *T. loquax* occurs south of Honduras and ranges as far as the south-central Caribbean slope of Costa Rica (Duellman 1970; Savage 2002; Köhler 2011; Amphibiaweb 2022).

In October 2018, Donald Varela-Soto encountered two adult individuals of a small green tree frog species that could not be attributed to any previously known similar species. The frogs were found in a regenerating wetland on private property in the Tapir Valley Nature Reserve, located in the northern Caribbean lowlands of Costa Rica between Tenorio and Miravalles volcanoes. Since his initial discovery, the research team has studied these frogs during targeted surveys that support the ongoing ecological restoration efforts in the reserve. Here we provide morphological, phylogenetic, and bioacoustic data that support the recognition of this striking green frog as a new species, and present information on its habitat and reproduction.

Materials and methods

Collected specimens were euthanized following accepted protocols. Fresh liver tissue of two specimens was removed for genetic analysis. Voucher specimens were fixed in 10% formalin, stored in 70% ethanol and deposited at the Museo de Zoología of the Universidad Nacional (ECB), Museo de Zoología of the Universidad de Costa Rica (UCR), and the Peabody Museum of Natural History at Yale University (YPM).

Amplification and sequencing. We extracted genomic DNA from fresh liver samples, using an AutoMate Express™ Instrument (Applied Biosystem) and PrepFiler Express™ Kit Protocol following the manufacturer's protocols. Conventional polymerase chain reaction (PCR) was carried out with the extracted DNA to amplify the 12S mitochondrial rRNA (12S) region with the primers: 5'-AAA CTG GGA TTA GAT ACC CCA CTA T-3', 5'-GAG GGT GAC GGG CGG TGT GT-3', and large subunit ribosomal RNA (16S) regions with the primers: 5'-CGC CTG TTT ATC AAA AAC AT-3' and 5'-CCG GTC TGA ACT CAG ATC ACG T -3'. The PCR amplifications were performed using a HotStarTaq® Master Mix Kit (QIAGEN). Amplifications were run with a total volume of 25 µL, which contained 12.5 µL of HotStarTaq Master Mix Kit (contains 2500 units HotStarTaq DNA Polymerase PCR Buffer with 3 mM MgCl₂, and 400 µM of each dNTP), 2µL forward and reverse primers (c. 50 ng/µL), 3 µL DNA template (c. 16 ng/µL) and 5.5 µL of Nuclease-free water. PCR conditions were as follows: 16S—an initial cycle of 5 min at 94°C, followed by 35 cycles of 45 sec at 94°C, 30 sec at 55°C, 45 sec at 72°C, plus a final cycle of 3 min at 72°C; 12S—an initial cycle of 2 min at 94°C, followed by 33 cycles of 30 sec at 94°C, 30 sec at 49°C, 60 sec at 65°C, plus a final cycle of 3 min at 72°C. DNA concentration was quantified using a Qubit® 3.0 fluorometer (Thermo Fisher Scientific). Amplified DNA fragments were sequenced using the Sanger platform. Samples were bidirectionally sequenced and PCR products were purified from agarose gel using a QIAquick gel extraction kit (Qiagen) per the manufacturer's instructions. Sequencing reactions were performed with a BigDye® Terminator cycle sequencing kit v3.1 (Applied Biosystems, Foster City, CA, USA) using each primer at a concentration of 0.5

µM and 10 µl of purified PCR products, with concentrations between 15–25 ng/µl for a 20 µl total volume reaction. The sequencing products were purified with BigDye XTerminator™ Purification Kit (Applied Biosystems) and subsequently analyzed with a SeqStudio genetic analyzer (Applied Biosystems).

Phylogenetic analyses. We compared 12S and 16S sequences of the new species with homolog sequences of the four known species of *Tlalocohyla* and other species included in the tribe Hylini (see Faivovich *et al.* 2018 for GenBank accession numbers). Using Faivovich *et al.* (2018) molecular database as starting ground, we restricted our gene sampling to 12S and 16S—for our goal was only to provide generic assessment for our samples. We also restricted taxon sampling to terminals for which both 12S and 16S sequences were available. Selected sequences were then aligned using the algorithm ClustalW (Thompson *et al.* 1994) implemented in the GUIDANCE2 Server (Sela *et al.* 2015). The alignment of 143 sequences was made with 398 bp from 12S and 570 bp from 16S, saved in fasta format, corrected to standardize the length of the sequences deleting external bases and converted to nexus format with the MEGA 5 program (Tamura *et al.* 2011). (Suppl. mat. 1). The “Models” tool from the MEGA 5 program was applied to find the evolutionary model that best explains the variation between these sequences. The best substitution model was Gamma distributed with invariant sites (GTR+G+I) for 12S and 16S, so that no partition strategy was applied. The phylogenetic analysis was carried out using both Bayesian inference and Maximum likelihood. For the Bayesian method we used MrBayes 3.2 (Huelsenbeck & Ronquist 2001), running 2 million generations using the Monte-Carlo Markov chain method, eliminating the first 500,000 trees prior to calculating the consensus tree, and a final standard deviation of less than 0.02 was obtained (Ronquist & Huelsenbeck 2003). Maximum likelihood was made using the MEGA 5 program with bootstrap method, applying 2000 replications. Trees were viewed and edited with FigTree (Rambaut 2014) and were rooted with *Phrynomedusa dryade* of the subfamily Phyllomedusinae. Uncorrected p-distances of the 16S fragments in the genus *Tlalocohyla* were calculated in MEGA 5. Newly generated sequences were deposited in GenBank under accession numbers OM749742-OM749745.

Measurements. We used fifteen measures of morphometric characters (in millimeters) described in Kok & Kalamandeen (2008), Watters *et al.* (2016) and Novaes-e-Fagundes *et al.* (2021): SVL (snout–vent length), HL (head length), HW (head width), ED (eye diameter), IND (internarial distance), EN (eye–nostril distance), NS (snout–nostril length), IOD (interorbital distance), TD (tympanum diameter), HAL (hand length), THL (thigh length), TL (tibia length), FL (foot length), Fin3DW (finger III disc width), and Toe4DW (toe IV disc width). SVL, HL, HW, HAL, TL, and FL were measured with a Total vernier caliper (precision 0.05 mm); all other variables were measured using a digital micrometer in an Olympus SZX7 stereomicroscope. Six standard ratios utilized by Duellman (1970): HL/SVL, HW/SVL, IND/HW, FL/SVL, TD/ED, and TL/SVL, and four additional ratios used by Novaes-e-Fagundes *et al.* (2021): Fin3DW/TD, ED/HW, ED/SVL, and HAL/SVL, were established. Because TD could not be consistently ascertained in all specimens examined, we also included Fin3DW/ED in our analysis.

Standards for dorsal outline and profile of the snout follow Heyer *et al.* (1990) and Duellman (2001), respectively. The interdigital webbing formula follows Savage & Heyer (1967) as modified by Myers & Duellman (1982) and Cisneros-Heredia & McDiarmid (2007). Sex was determined by the presence/absence of oocytes as well as secondary sexual characters (i.e., nuptial pads, vocal slits, and vocal sacs; present only in males). Nuptial pad structure was assigned according to Luna *et al.* (2018). Body color pattern, shape of head and texture of skin was assigned according to Kok & Kalamandeen (2008). Color descriptions for the holotype follow Köhler (2012). We examined several uncollected individuals of the new species from Tapir Valley Nature Reserve in addition to the type series, and compared their external features with those of other *Tlalocohyla* species and with members of morphologically similar genera, using data obtained from the literature (Duellman 1970, Savage 2002). General body morphology was described according to Duellman (2001).

Bioacoustics. We analyzed 28 advertisement calls obtained between December 2020 and May 2021 from seven unique, uncollected males. Calls were recorded using Iphone 8 and Iphone 6 cellular phones, and a Canon PowerShot SX740 HS digital camera. The recorders were positioned between 30–50 cm from each calling male. Recordings were obtained in MP4 format and converted to WAV format for analysis. All recordings and metadata are archived in the Collection of Records of the Fonoteca Zoológica (www.FonoZoo.com FZ-SOUND-CODE: 14163-14169). We follow the call-centered scheme definitions suggested for describing anuran vocalizations in Köhler *et al.* (2017). In each recorded advertisement call we measured the following parameters: call duration, inter-call interval, call repetition rate, number of notes per call, note duration, note repetition rate, inter-note interval, call amplitude, pulses per note, dominant frequency and bandwidth. Call parameters were analyzed in RAVEN 1.4 (Bioacoustics Research Program 2015). All parameters were measured from values observed in the program’s selection spectrum view

tool table. RAVEN 1.4 parameters were set as follows: Hann window type function, window size of 1024 samples, 3 dB filter bandwidth of 61.9 Hz, time grid 90% overlap, time grid size of 102 samples, 43.1 Hz frequency grid spacing. We compared our recordings with sound files of *T. picta* (FZ-SOUND-CODE: 8953) and *T. smithii* (FZ-SOUND-CODE: 7065, FZ-SOUND-CODE: 7270), and with the call descriptions and spectrograms provided for those species by Lee (1996) and Duellman (2001).

Description of the tadpole. Terminology for larval morphology follows Altig & McDiarmid (1999), with the exception of the position of the intestinal mass, which follows Faivovich (2002). Methylene blue was used to enhance visibility of oral disc structures. Nineteen measurements were recorded from 3 tadpoles in Gosner stages 33–34 (Gosner 1960) (Table 1). Twelve measurements follow Lavilla & Scrocchi (1986): TL (total length), BL (body length), TAL (tail length), MTH (maximum tail height), TMH (tail muscle height), BH (body height), BW (body width), ED (eye diameter), ODW (oral disc width), END (eye-nostril distance), NSD (nostril to type of snout distance), and ND (nostril diameter); four measurements follow Altig & McDiarmid (1999): TMW (tail muscle width), IND (internal distance), IOD (interorbital distance), and SS (distance of snout to center of spiracle); two measurements follow Grosjean (2005): DFH (dorsal fin height) and VFH (ventral fin height); and one follows Araujo-Vieira *et al.* (2015): SL (spiracle length). Measurements (in millimeters) were taken using a digital micrometer in an Olympus SZX7 stereomicroscope except TL, BL, and TAL, which were measured with a Total vernier caliper (precision 0.05 mm).

TABLE 1. Measurements (in mm) and ratios of the type series (including the holotype in bold) of *Tlalocohyla celeste* sp. nov. See Materials and methods section for the abbreviations of measurements.

Measurements	UCR 23700	ECB-Anf-f50-08-01,01.	YPM 13222	UCR 23701
Sex	Male	Male	Male	Female
SVL	20.10	20.15	21.45	24.55
HL	7.700	7.550	8.350	8.300
HW	7.350	6.950	7.650	8.500
HAL	6.650	6.200	6.300	6.900
THL	10.30	9.400	10.60	11.95
TL	11.45	10.45	11.40	13.30
FL	8.750	8.450	8.850	10.30
ED	2.142	2.609	2.542	2.711
IND	1.894	1.898	2.098	2.352
EN	1.888	1.984	2.169	2.487
NS	1.313	1.137	1.071	1.365
IOD	3.267	2.838	3.008	3.673
TD	0.492	0.817	0.709	0.819
Toe4DW	0.750	0.549	0.750	0.941
Fin3DW	0.553	0.829	1.236	1.160
HL/SVL	0.383	0.375	0.389	0.338
HW/SVL	0.366	0.345	0.357	0.346
IND/HW	0.258	0.273	0.274	0.277
FL/SVL	0.435	0.419	0.413	0.420
TD/ED	0.230	0.313	0.279	0.302
TL/SVL	0.570	0.519	0.531	0.542
Fin3DW /TD	1.124	1.015	1.743	1.416
ED/HW	0.291	0.375	0.332	0.319
ED/SVL	0.107	0.129	0.119	0.110
HAL/SVL	0.331	0.308	0.294	0.281
Fin3DW/ED	0.258	0.318	0.486	0.428

Results

Phylogenetic analyses. The resulting data matrix had a total sequence length of 968 bp, 398 bp for 12S and 570 bp for 16S. The phylogenies inferred by Mr.Bayes and MEGA 5 show that *Tlalocohyla* is a well-supported clade, which is nested within a clade which includes *Isthmohyla*, *Hyla*, *Tripurion* and *Smilisca* (the Hyline tribe sensu Faivovich *et al.* 2018; although our topology is radically different see discussion). All phylogenetics analysis supported the inclusion of the new species in the genus *Tlalocohyla* (Fig. 1; Suppl. fig. 2–3). Although there are clear differences in the overall topology of the Bayesian and ML analyses, both show three clades within the genus *Tlalocohyla* (*T. smithii* + *T. picta*; *T. celeste*; *T. loquax* + *T. godmani*), although supports are overall low. While our Bayesian model recovers our samples all belonging to a species sister to a clade composed of *T. godmani* and *T. loquax*, and all these sister of a clade composed of *T. smithii* and *T. picta* (Fig. 1; Suppl. fig. 2), our ML tree recovers a polytomy between *T. smithii* + *T. picta*, *T. celeste*, and *T. loquax* + *T. godmani* (Suppl. fig. 3). The integrative interpretation of topological results with other data (size, morphology, calls, behavior, distances p, etc.) allows us to conclude that this lineage is distinct from all other lineages. Thus, we describe it as a new species below.

Species account

Tlalocohyla celeste sp. nov.

Tapir Valley Tree Frog, Rana Arbórea del Valle del Tapir

(Figures 2–7)

Holotype. UCR 23700, an adult male from Costa Rica, Alajuela, Upala, Bijagua, Tapir Valley Nature Reserve (10.72° N, 85.01° W; 660 m asl), collected on September 13, 2021, by Juan G. Abarca, Valeria Aspinall, Donald Varela, and Esteban Brenes.

Paratopotypes. Two adult males, ECB-Anf-f50-08-01,01 and YPM 13222, same data as holotype; UCR 23701, an adult female collected by Donald Varela on September 15, 2021.

Generic placement. Bayesian (Fig. 1, Suppl. fig. 2) and Maximum likelihood analyses (Suppl. fig. 3) confirm the inclusion of the new species in the genus *Tlalocohyla*.

Diagnosis. The new species can be diagnosed by the following combination of traits: (1) small size (adults males: 21 mm, females: 24 mm of SVL; n=4); (2) tympanic membrane not-evident; (3) vocal sac developed, single, subgular, extending to the pectoral region; (4) vomerine teeth absent; (5) dorsal color yellow-green (#103); (6) ventral skin transparent; (7) white peritoneum covering all internal organs; (8) presence of an incomplete sulfur white (#96) dorsolateral stripe that originates at the posterior edge of the orbit and extends posteriorly to a point more than halfway towards the insertion of each hindlimb, bordered above for its entire length by a diffuse mahogany red (34) stripe that extends anteriorly towards the tip of the snout; (9) presence of a small light cyan (#158) axillary membrane.

Within its genus, *Tlalocohyla celeste* can be differentiated from *T. godmani* and *T. loquax* by the following characteristics (condition for *T. celeste* in parentheses): maximum SVL 45 mm (24 mm); venter pale lemon yellow or creamy yellow (transparent ventral skin) and extensive axillary membrane (very small axillary membrane). *Tlalocohyla celeste* is similar in overall appearance to *T. smithii* and *T. picta*, but can be differentiated based on the following characteristics: from *T. smithii* by its smaller size, maximum SVL 30 mm (24 mm); pale yellow, tan or brilliant yellow dorsum (bright yellow-green with mahogany red spots); a thin complete white or cream dorsolateral stripe that is usually bordered below by a thin brown line (an incomplete sulphur white dorsolateral stripe bordered above by a diffuse mahogany red stripe); white belly (transparent); vomerine teeth present (absent); and from *T. picta* by the relatively uniform yellowish tan dorsal coloration (bright yellow-green with mahogany red spots); presence of a complete white or cream dorsolateral stripe that may be bordered below by a poorly defined reddish, brown or gray band (an incomplete sulphur white dorsolateral stripe bordered above by a diffuse mahogany red stripe); white bones (green bones) and vocal sac yellow (brilliant light cyan). *Tlalocohyla celeste* also differs from these two species in its advertisement call and tadpole morphology (see below).

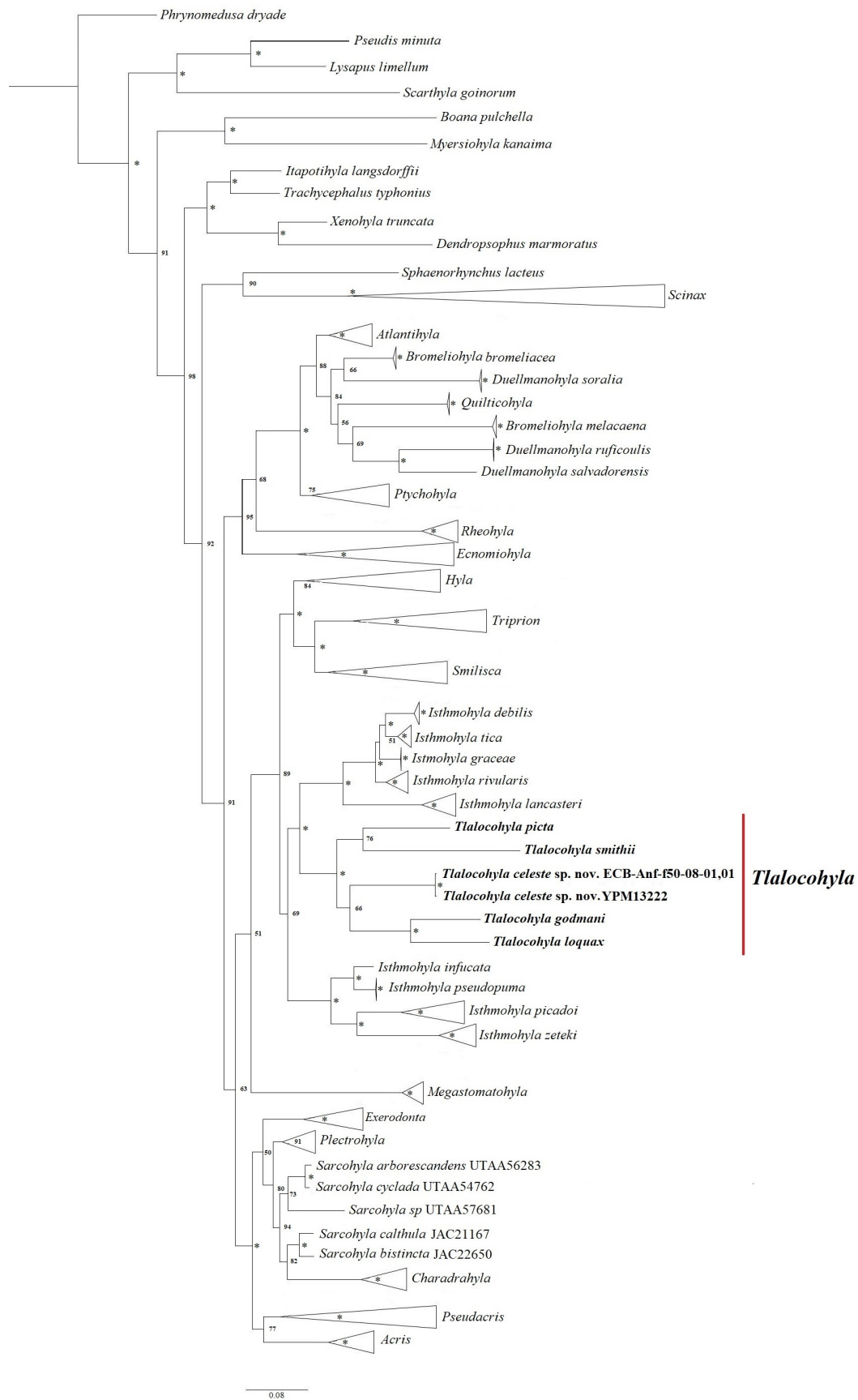


FIGURE 1. Bayesian phylogenetic tree within the Hylidae family based on 12S and 16S mitochondrial DNA genes. Posterior probabilities in nodes, asterisks represent support of >95. Branches are collapsed to illustrate genus-level relationships, see expanded branches on Suppl. material. 2. The scale bar refers to the estimated substitutions per site.

Tlalocohyla celeste is among the smallest hylids in Costa Rica, slightly smaller than *Isthmohyla zeteki*, and may be confused with other small hylid species present within its range. Members of the genus *Dendropsophus* are small tree frogs with an axillary membrane but none are green in coloration with transparent ventral skin. *Scinax* species have a similar, rounded protruding lateral snout profile but are significantly larger in size and never have light dorsolateral markings. *Tlalocohyla celeste* is most likely to be confused with juveniles of the syntopic *Boana rufitela*, but the latter has a rounded snout in lateral profile and its white dorsolateral lines are complete, extending from the snout tip backwards to the vent, passing over top of the hindlimbs. These light markings fade and eventually disappear completely as young *B. rufitela* mature. Because of its bright green coloration and transparent ventral skin, *T. celeste* may be mistaken for a glass frog (family Centrolenidae), however glass frogs invariably lack a pattern of light dorsolateral stripes.

Description of holotype. An adult male with a SVL of 20.10 mm (Fig. 2), in a good state of preservation, head slightly longer than wide, HL 38.3%, and HW 36.5% of SVL. Snout nearly rounded in dorsal view, rounded protruding in profile. Nostrils rounded, dorsolateral, directed laterally, located on slightly raised processes, IND 25.8% of HW. Canthus rostralis well defined and rounded. Loreal region concave. Eyes large and protuberant, ED 39.1% and 10.7% of HW and SVL, respectively. Pupil horizontally elliptical. Tympanum small, TD 23.0% of ED, tympanic membrane inevident, but tympanic annulus visible through the skin (Fig. 3C), tympanum matches character combination number 2 in Lynch and Duellman (1997). Tongue ovoid, free laterally and posteriorly. Texture of tongue granular. Premaxillary and maxillary teeth present, no vomerine teeth visible between choanae. Choanae rounded anteriorly and widely separated. Vocal apertures are slit-like and elongated, nearly parallel the mandible. Vocal sac single and subgular, extends posteriorly to the pectoral region (Fig. 2B and Fig. 7).

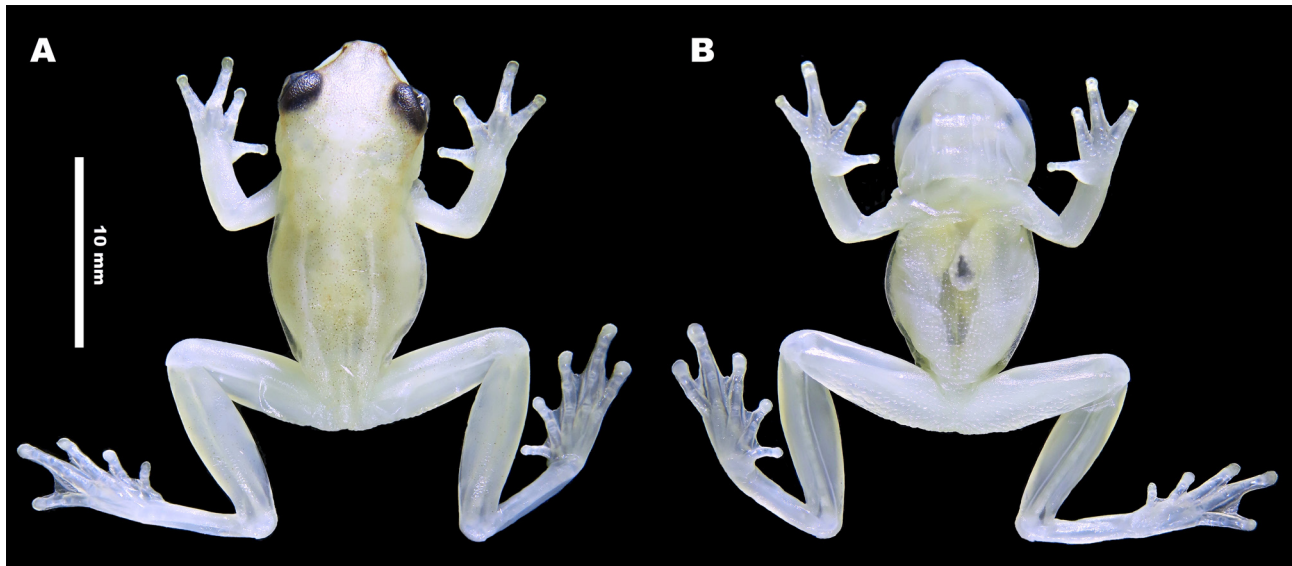


FIGURE 2. Holotype of *Tlalocohyla celeste* sp. nov. (UCR 23700). (A) Dorsal view. (B) Ventral view.

Forelimbs not hypertrophied, upper arms and forearms slender, consistent throughout in its thickness. Hands proportionally large, HAL 33.1% of SVL. Lacks ulnar skin fold. A small axillary membrane present. Fingers robust, relative finger length I<II<IV<III. Discs moderately expanded and round (Fin3DW 25% of ED). Finger discs are comparable in size but finger disc I is slightly smaller than others. Subarticular tubercles single, rounded or globose, large and slightly bifid in fingers III and IV. Supernumerary tubercles large, single and rounded. Accessory palmar tubercles numerous, rounded, large and globular; span the entire palmar area in a tightly packed way. Inner metacarpal tubercle (thenar) elongated, elliptical, globular and large; outer metacarpal tubercle (palmar) not clearly differentiated from the accessory palmar tubercles. White smooth nuptial pads without epidermal projections, at the base of the first finger, formed by a grouping of glandular acini, each circular or ovoid in shape (Fig. 6C). The interdigital membrane between fingers I–II is vestigial, but it is slightly more developed between fingers II–III–IV. Webbing formula I3+–2- II 2– 3-III3- –2-IV.

Hind limbs slender, THL slightly greater than FL and slightly smaller than TL. TL of about 57.0% of SVL, FL 43.5% of SVL. Toes robust. Relative length of toes I<II<III<V<IV. Discs rounded and expanded. Subarticular tubercles single, rounded and globular. Supernumerary tubercles small, single and rounded. Inner metatarsal tubercle

medium-sized, elliptical; outer metatarsal tubercle absent. Webbing formula I 2⁻-2⁺II 1^{1/2}-3⁺ III 1^{1/2}-3⁻ IV 2⁺-1^{1/2} V, free parts of toes fringed. Cloacal dermal fold absent.

Body covered in smooth skin throughout, except for the central region of the venter and the undersides of the thighs where skin texture is distinctly granular (Fig. 6A).

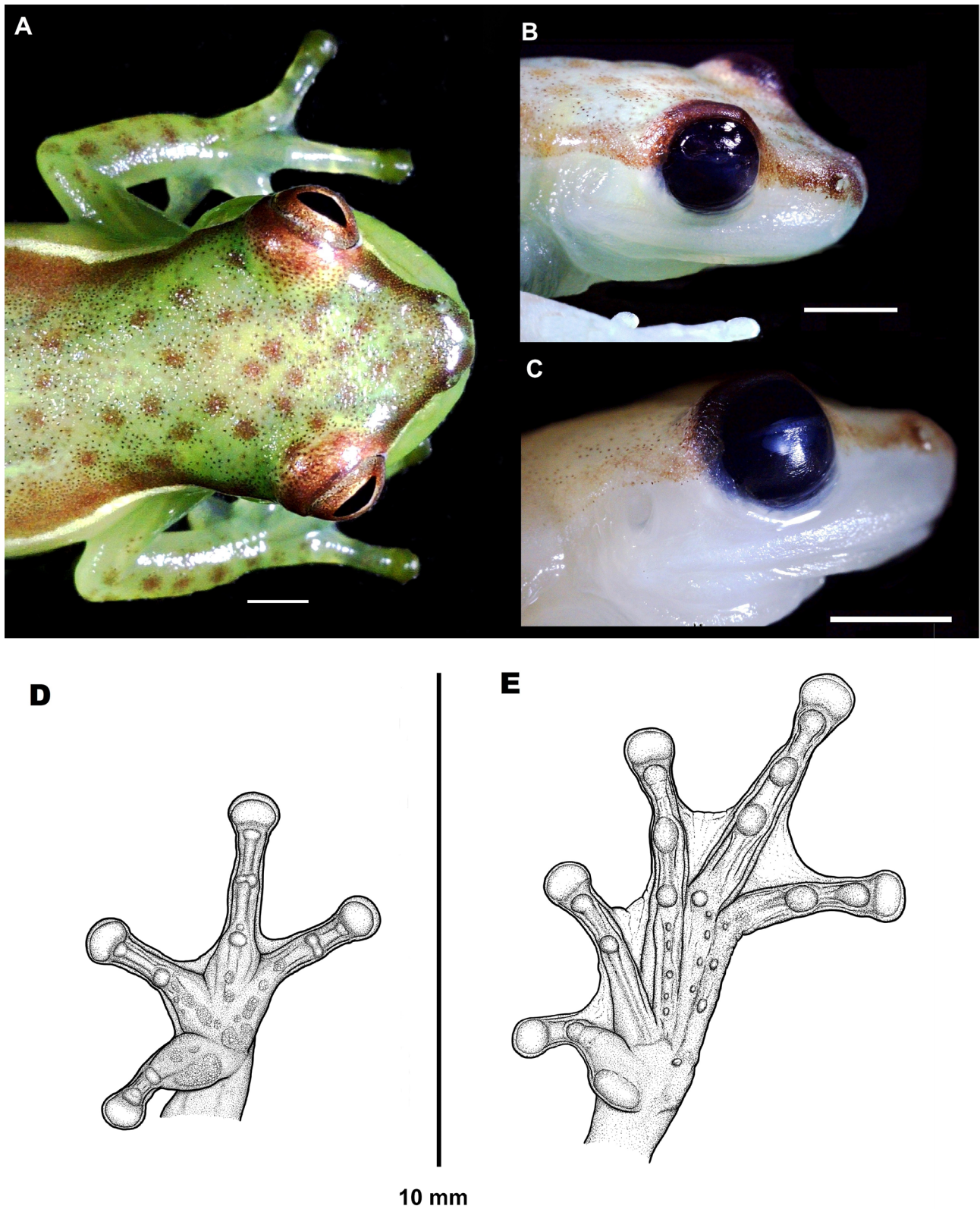


FIGURE 3. Holotype of *Tlalocohyla celeste* sp. nov. (UCR 23700) (A) Dorsal view of head in living specimen. (B) Lateral view of head in preserved specimen. (C) Lateral view in preserved specimen, note the tympanum. Scale bar = 2 mm. (D) Right hand in ventral view. (E) Right foot in ventral view.



FIGURE 4. Variation in dorsal pattern of *Tlalocohyla celeste* sp. nov. (A–B) male holotype of *Tlalocohyla celeste* sp. nov. (UCR 23700) in life. (C) Size differences between females and males. (D) Typical nocturnal pattern of males. (E) Female with the oocytes visible by transparency in the body. (F) Diurnal pattern of adults, males and females, note the white iris chance. (G) Juvenile. (H) Diurnal pattern with red-brown iris.

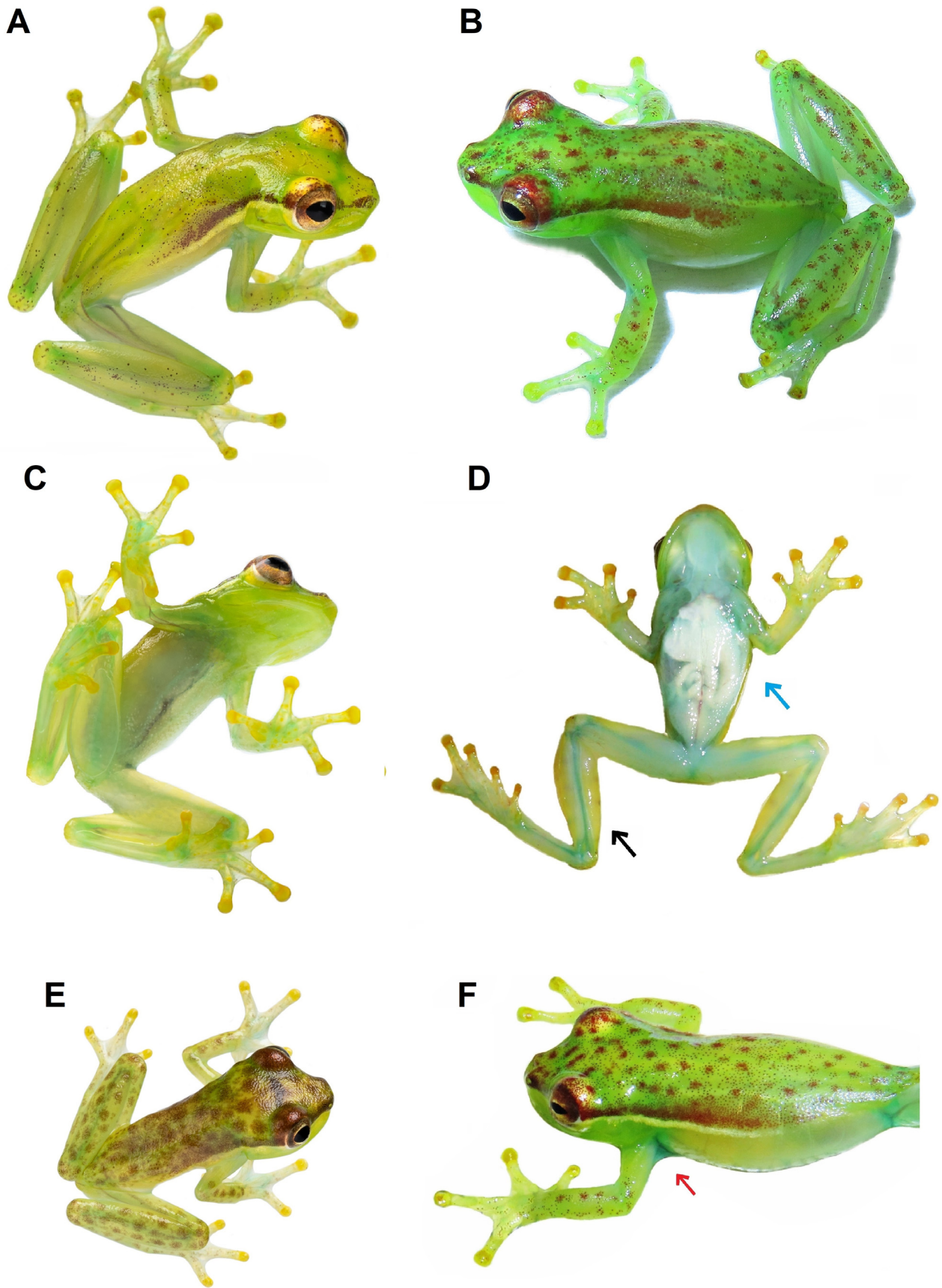


FIGURE 5. Variation and diagnostic characteristics in *Tlalocohyla celeste* **sp. nov.** (A-B) pattern change and green tones change of two uncollected males. (C) Ventral view in diurnal pattern. (D) ventral view of female (UCR 23701), note green bones (black arrow) and white peritoneum (blue arrow). (E) Spotted pattern in juvenile. (F) Axillary membrane (red arrow).

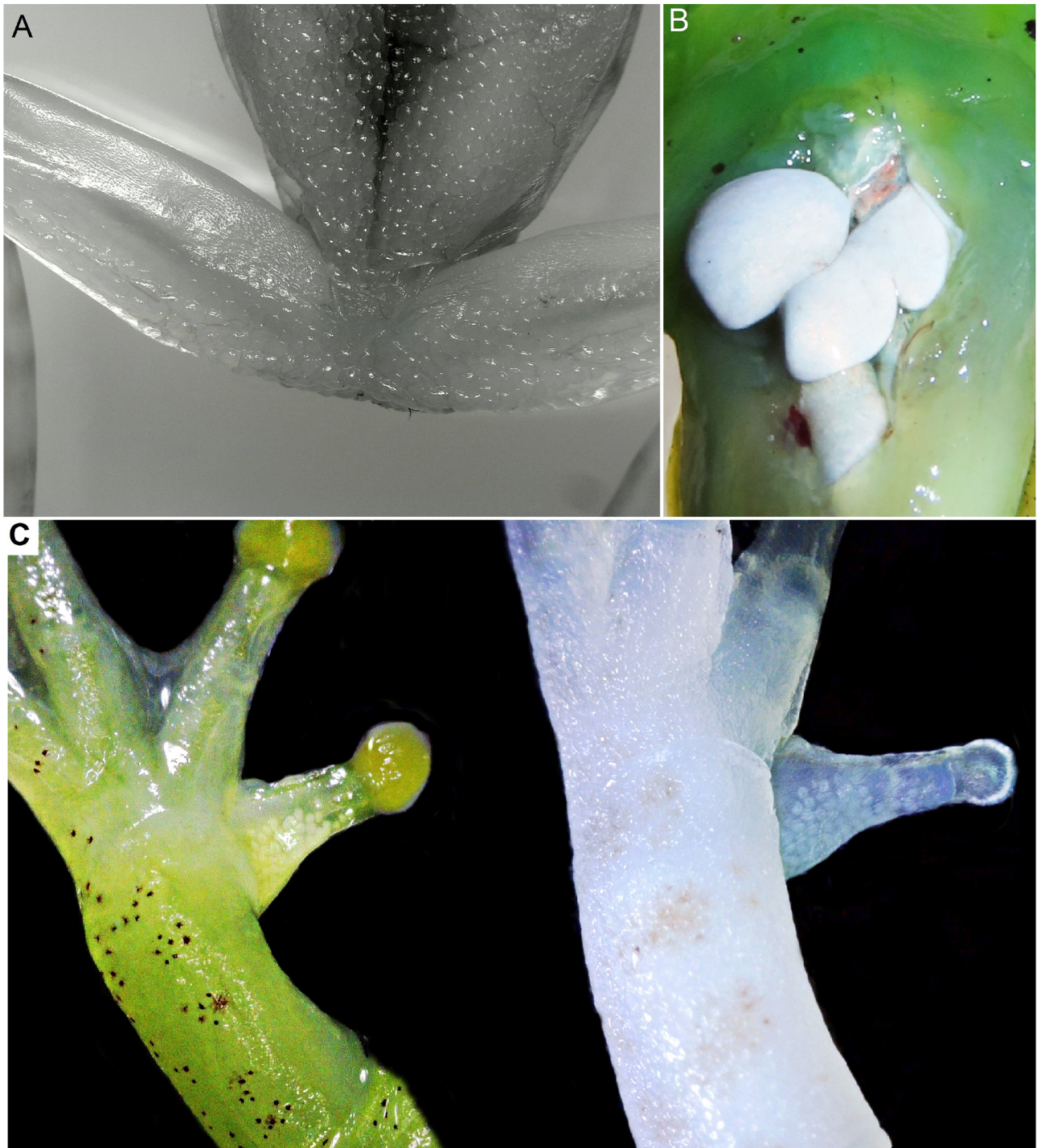


FIGURE 6. Ventral view *Tlalocohyla celeste* sp. nov. (A) Ventrals skin texture, and cloacal view. (B) Liver of recently preserved specimen (ECB-Anf-f50-08-01,01.). (C) Nuptial pads of the left hand in *Tlalocohyla celeste* sp. nov. male holotype (UCR 23700), in life, and preserved.

Measurements of the holotype (in mm). SVL 20.10; HL 7.70; HW 7.35; IND 1.89; IOD 3.26; ED 2.14; EN 1.88; TD 0.49; HAL 6.65; FL 8.75; TL 11.45; Fin3DW 0.55; Toe4DW 0.75.

Coloration of the holotype in life (nocturnal coloration). Background color of head, upper back and limbs brilliant yellow-green (#103), with numerous mahogany red (#34) blotches relatively evenly dispersed over the dorsal surfaces of the head, body and lower limbs (Fig. 4A–B). A narrow sulfur white (#96) dorsolateral stripe starts behind each eye and extends towards the insertion of each hind limb, gradually fading out near a point about halfway down the body. A relatively poorly defined mahogany red stripe extends from the tip of the snout along

the canthal region, and continues post-ocularly following the upper border of the sulfur white dorsolateral line; it gradually fades out at the same point as the light stripe. Lateral surfaces of the body and head, below the dorsolateral lines, lack mahogany red spots. Upper surfaces of finger and toe tips light greenish yellow (#87). Upper edge of orbit Pratt's rufous (#72); remainder of upper eyelid suffused with spectrum yellow (#79). Posterior and anterior edge of orbit bordered by a narrow white line. Iris gold with raw umber (#23) reticulations. Vocal sac yellow-green (#103) when deflated, turquoise green (#147) when inflated. Skin covering ventral surfaces transparent, allowing muscles, veins, bones, and intestines to be visible (Fig. 5C–D). Internal organs black, but hidden from view by an opaque, white peritoneum (Fig. 6B).

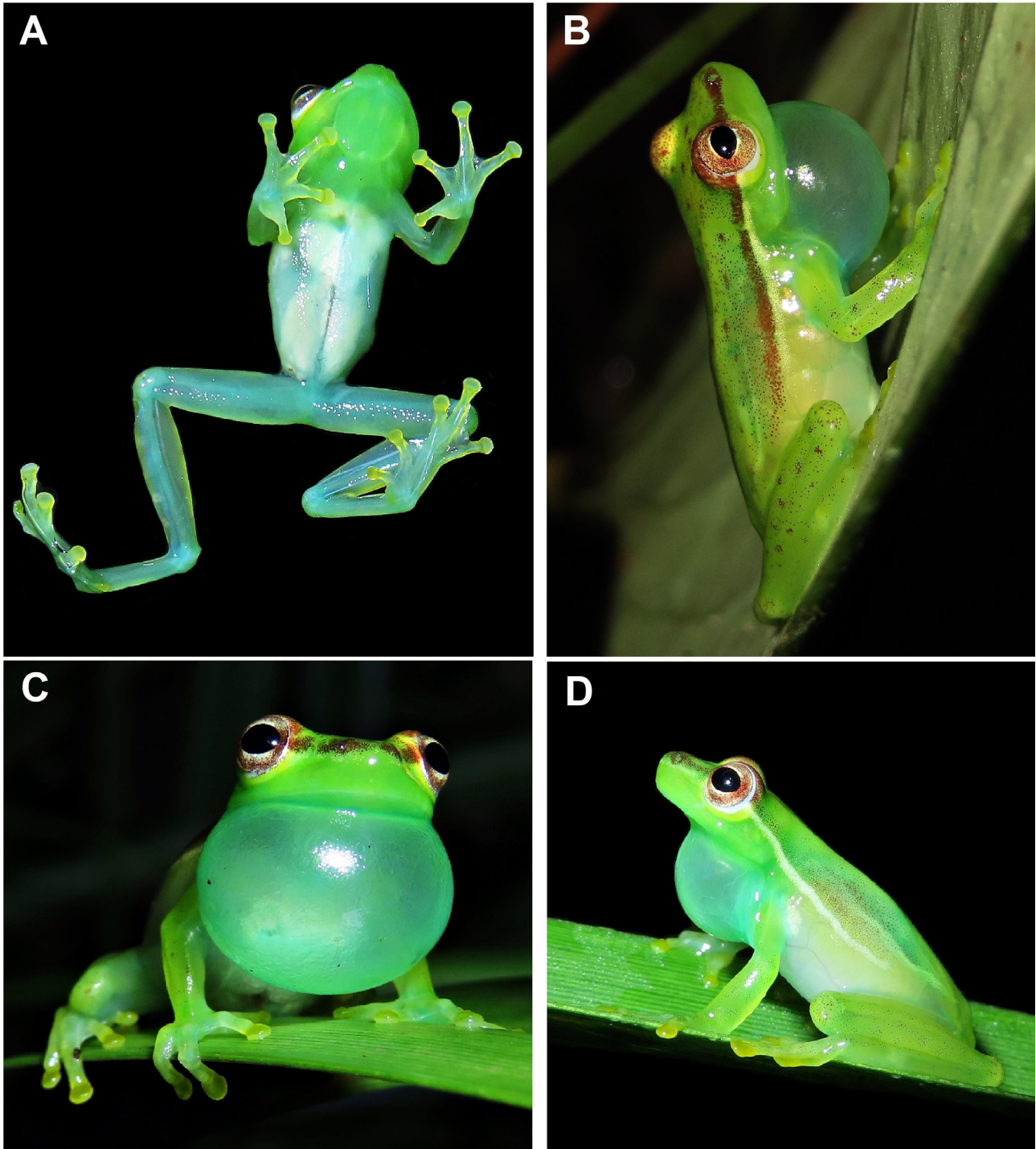


FIGURE 7. Vocal sac of uncollected males of *Tlalocohyla celeste* **sp. nov.** (A) Ventral view and vocal sac deflated. (B–D). Calling males perched on vegetation in different positions, note the vocal sac extension.

Coloration of the holotype in preservative. In formalin, yellow-green dorsal coloration becomes pale greenish white (#97), while mahogany red markings (dorsolateral lines and dorsal spots) turn pale vinaceous (#247). The color pattern fades in a similar fashion after ethanol preservation, leaving dorsolateral markings and dorsal spots faded but visible (Fig. 2). The iris becomes black (Fig. 3). Hands, feet, and tips of digits fade to a uniform creamy-white. Skin on ventral surfaces retains some transparency in preservative.

Variation. Morphometric variation is detailed in Table 1. Females are larger than males (Fig. 4C) and lack nuptial pads, vocal slits and a vocal sac. The paratopotypes are comparable in coloration to the holotype. There is a noticeable difference between nocturnal (Fig. 4D) and diurnal coloration (Fig. 4F) in this species, especially in the intensity and visibility of the mahogany red dorsal spots and dorsolateral lines. These markings are less prominent during the day, causing the dorsal pattern to appear more uniformly green and less spotted. In addition, the eye color brightens during the daytime to a lighter silver-gray (Fig. 4F). The presence of blue green bones, lymph, and other tissues (Fig. 5) indicates that this species has physiological chlorosis, a trait that has been documented in other arboreal frogs (Taboada *et al.* 2020).

TABLE 2. Measurements (in mm) of the tadpoles of *Tlalocohyla celeste* sp. nov. See Materials and methods section for the abbreviations of measurements.

Measurements	Stages 33-34 (N = 3)		
	1	2	3
TL	26.6	26.1	29.7
BL	10.6	9.4	10.3
TAL	14.9	20.8	21.0
MTH	5.68	4.53	5.61
TMH	2.93	2.92	2.55
TMW	2.63	2.85	1.89
BH	5.50	5.59	5.09
BW	6.54	6.51	5.42
ED	1.44	1.47	1.11
ODW	2.99	2.54	2.31
END	2.07	1.95	1.68
NSD	1.33	1.85	1.34
ND	0.54	0.32	0.43
IND	2.59	2.06	1.95
IOD	4.47	4.11	4.55
DFH	1.77	1.47	2.24
VFH	1.47	1.06	1.44
SL	1.56	1.50	1.36
SS	6.44	6.13	5.15

Metamorphs and small juveniles exhibit a lighter green dorsum and lack the light dorsolateral stripes during early developmental stages (Fig. 11B–C). The small, light cyan axillary membrane (Fig. 5F) is not seen in juveniles. Such young individuals generally display clusters of mahogany red blotches on the dorsum, most densely concentrated anteriorly but with considerable variation in their aggregation patterns. A broad, dark canthal stripe and short postocular stripe are usually present in juveniles, while the dorsal surfaces of the head, body, and limbs are marked with bold dark brown to purplish-brown spots. Dark-colored spots and stripes lighten ontogenetically likely to transform into the adult color pattern as the frogs age (Fig. 4G, 5E and 11D).

Tadpole description. Tadpoles of *Tlalocohyla celeste* (Fig. 11A and Fig. 12) in Gosner stages 33–44 conform to the following description: body depressed (BH/BW=0.87–0.94), ovoid in dorsal view and ovoid or elliptical in lateral view, from 0.35–0.40 times the TL. Snout rounded in dorsal and lateral aspects. Eyes medium-sized (ED/BL=0.11–0.16), laterally located, visible in ventral view. The nostrils are situated approximately midway between the eyes and the tip of the snout. Nares rounded, medium-sized (ND/BL=0.03–0.05), dorsally located and dorsally

directed. Well-developed fleshy flanges on the marginal rim. Spiracle sinistral, lateral, directed posterodorsally, and located on the posterior third of the body. Spiracle opening small (SL/BL=0.13–0.16). The intestinal mass is positioned perpendicular to the longitudinal body axis and visible through the clear ventral skin. The cloacal tube is short, dextral and has a triangular apex.

The small oral disc (ODW/BW=0.39–0.46) is positioned anteroventrally. Oral disc not emarginated; has a single row of short marginal papillae with a small anterior gap. Several submarginal papillae are randomly distributed laterally in the oral disc (Fig. 12D). LTRF 2(2)/3; A-1 and A-2 of equal size; A-2 with a narrow medial gap; P-1 equal in size to P-2; P-3 approximately one quarter the size of P-1 and P-2. Jaw sheaths small, measuring less than half of the oral disc; finely serrated along their entire margin. Anterior jaw sheath smoothly arched, posterior jaw sheath shallowly V-shaped. Tail of intermediate height (MTH/TAL=0.21–0.38) with moderately robust musculature (TMH/BH=0.50–0.53); dorsal fin higher than ventral fin (DFH/VFH=1.20–1.56). Dorsal and ventral fins of intermediate height (DFH/TAL=0.07–0.11; VFH/TAL=0.05–0.09); dorsal fin initiates on the body at a point slightly anterior to the base of the tail; maximum fin height is achieved near the midpoint of the tail's length. Ventral fin originates towards the end of the venter, anterior to the cloacal tube. The lateral line system is indistinct.

In life, the general color pattern of the body and tail musculature is pale cream, pale white or pale yellow, with small brown flecks on the dorsal surfaces (Fig. 11A–12). Dorsal surfaces of head yellow ochre (#14) to tawny olive (#17); lateral surfaces slightly lighter in hue, marked with concentrations of mahogany red (#34) to warm sepia (#40) spots. A pattern of relatively evenly-spaced, rounded warm sepia (#40) spots is a prominent feature of the dorsal surfaces; dorsal and lateral surfaces also display a fine dusting of irregular white or gold specks. A distinct, but poorly defined warm sepia (#40) stripe extends from a point near the anterior edge of the oral disc towards the eye and continues as an indistinct postocular stripe onto the body. Iris gold, marked on either side of the pupil with a warm sepia (#40) spot; both dark spots align with the dark eye stripe that originates at the snout tip. Ventral skin is transparent, revealing reddish hues anteriorly at the thoracic level and cream white (#52) coloration at the level of the intestines. Throughout the larval development period, the intestinal tract becomes increasingly suffused with black pigment. This ontogenetic change creates a striking black-and-white ventral pattern that contrasts sharply with the dorsal and lateral coloration. Tail fins are transparent, marked with black or raw umber (#23) blotches of irregular shape and size, as well as small white spots. Tail musculature is yellow ochre (#14) with black or warm sepia (#40) spots, occasionally with a fine black line on the medial side of the tail that can be intact or interrupted. Upon preservation in 10% formalin, the larval coloration fades to pale greenish white (#97), whereas the eye stripe, dorsal spots and tail markings become black.

Tadpoles of *Tlalocohyla celeste* differ most notably from other tadpoles in the genus as follows (Gosner stages in parenthesis): in tadpoles of *T. godmani* (38), *T. loquax* (26), and *T. picta* (38), the dorsal fin originates on the body at the level of, or anterior to the location of the spiracle (Lee 1996; Duellman 2001), whereas in *T. celeste* the dorsal fin originates at the base of the tail. Tadpoles of *T. smithii* (37) are most similar to those of *T. celeste* as their dorsal tail fin starts close to the tail base. However, tadpoles of *T. smithii* differ in having the posterior third of the tail black and the height of their dorsal fin is relatively constant throughout until it tapers to a fine tip (Caldwell 1986). Tadpoles of *T. celeste* lack a black tail tip and their dorsal fin increases in height towards the middle of the tail before tapering towards the tip.

Advertisement call. The vocal repertoire of *Tlalocohyla celeste* is composed of at least three call types. Call type I (Fig. 8A–C) is composed of a trill of notes, with average call duration of 0.34 s (0.30–0.39 s; n=17), emitted at intervals of 2–10 s (n=14) and average call repetition rate of 12 calls/minute. Call type I is composed of 9–13 notes, each note having average duration of 0.01 s (0.01–0.02 s; n=17), with a note repetition rate of 33.4 notes/s and inter-note interval of 0.01 s (0.01–0.02 s; n=17). Notes that comprise the call's trill-pattern can be modulated to increase amplitude towards the end of the call or display similar amplitude throughout (Fig. 8A). Call dominant frequency ranges 3.80–4.30 kHz (Fig. 8D). Bandwidth values range from 1.13 (0.90–1.40) to 13.0 (10.3–23.0) kHz (n=17). This call has several sparse harmonics and each pulsed note (30–50 pulses per note) displays an initial high amplitude pulse but subsequently decreases to lower amplitude pulses (Fig. 8E).

Call type II (Fig. 8F–I) is composed of one to three squeak-like modulated pulsatile notes, each note having an average duration of 0.08 s (0.07–0.10 s; n=4), with a note repetition rate of 3.4 notes/s and inter-note interval of 0.02 s (0.01–0.02 s; n=4). The dominant frequency ranges from 4.00–4.40 kHz, bandwidth values range from 0.85 (0.40–1.5) to 12.1 (11.2–14.6) kHz (n=4). Call type II usually was emitted 0.17–0.21 s (n=4) after call type I.

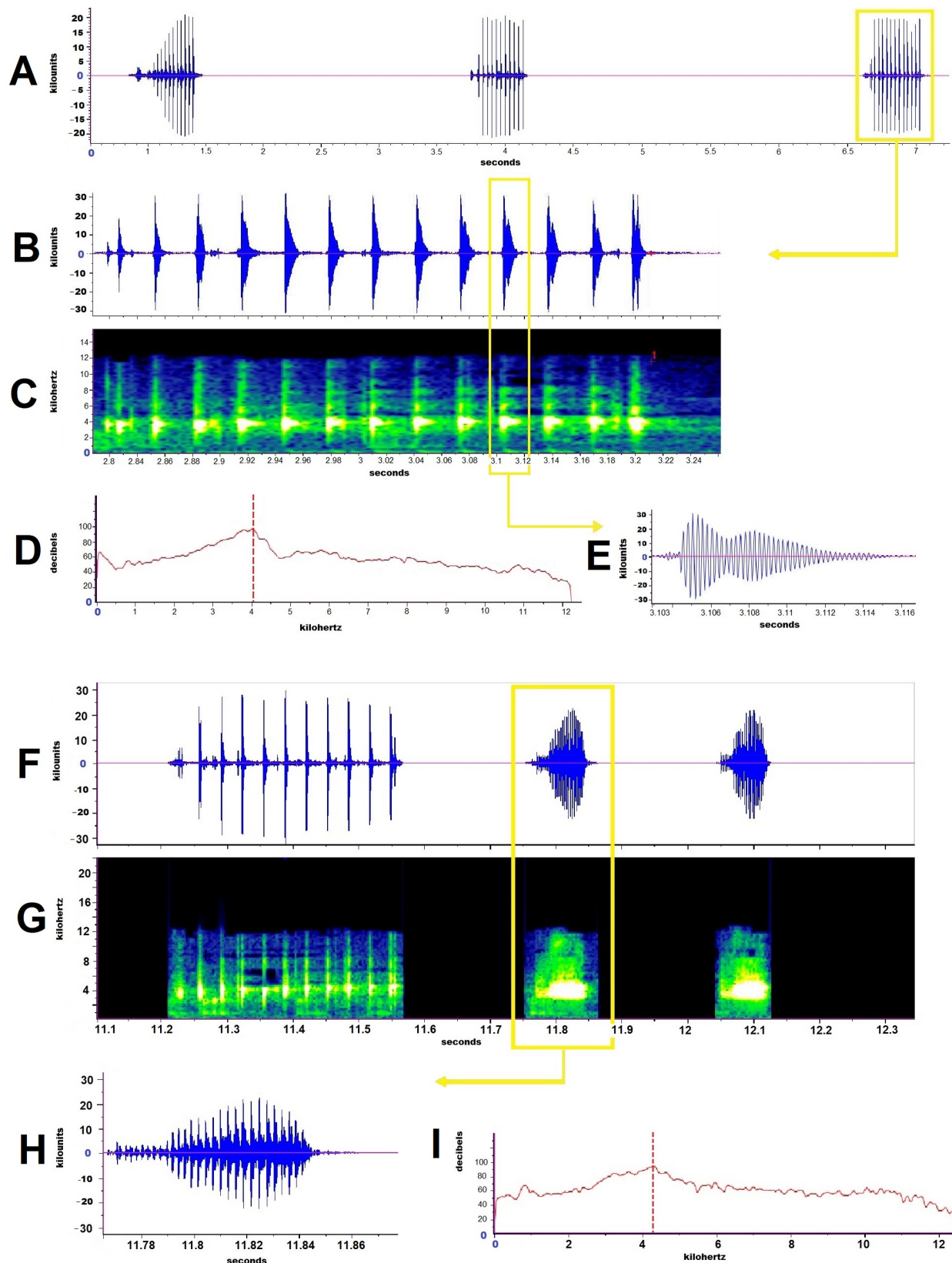


FIGURE 8. Calls repertoire of *Tlalocohyla celeste* sp. nov. **Call type I:** (A) oscillogram of a call series type I, first growing in amplitude and the second and third with similar amplitude notes; (B) oscillogram and (C) spectrogram of a call type I with 13 notes; (D) power spectrum and (E) oscillogram of a single note. **Call type II:** (F) oscillogram and (G) spectrogram of a call group: call type I following call type II; (H) oscillogram and (I) power spectrum of the single squeak-like note in call Type II. Dotted red line indicates the dominant frequency.

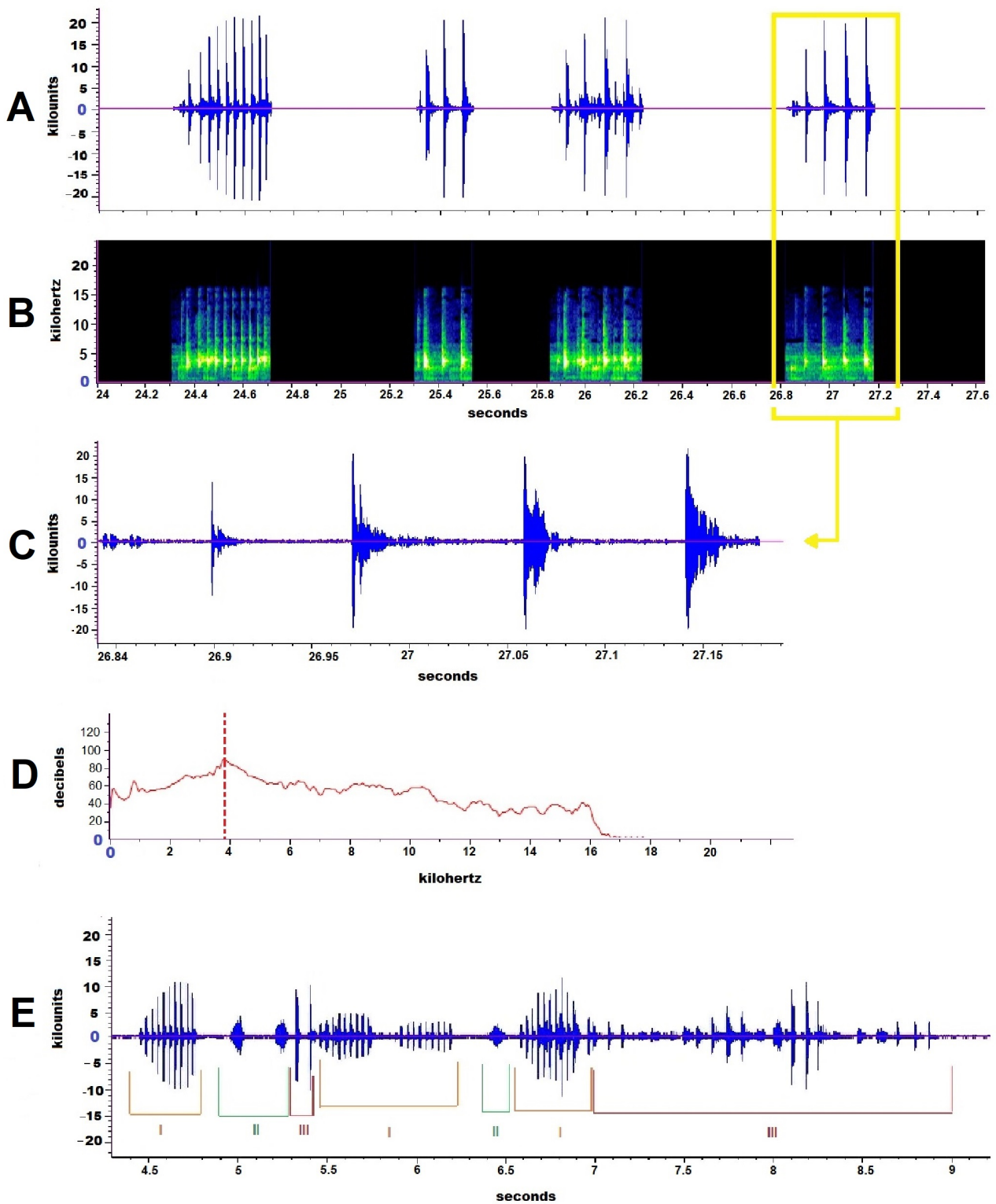


FIGURE 9. Call repertoire of *Tlalocohyla celeste* sp. nov. **Call type III:** (A) oscillogram and (B) spectrogram of a call series: call type I following call type III; (C) oscillogram and (D) power spectrum of notes in call type III. Dotted red line indicates the dominant frequency. (E) Oscillogram of call groups in *Tlalocohyla celeste* sp. nov. Showing a combination of the three call types (type I in orange, type II in green and type III in red) emitted by different males during the chorus.

Call type III (Fig. 9A–D) is a croak of pulsed notes with an average duration of 0.29 s (0.21–0.34 s; n=7), emitted at intervals of 0.35–1.61 s (n=7), with an average call repetition rate of 23 calls/s (n=7). Call type III is composed of 3–5 pulsed notes of modulated amplitude, with an average call duration of 0.29 s (0.21–0.34 s; n=7).

Each note has an average duration of 0.03 s (0.03–0.04 s; n=7), an inter-note interval of 0.04 s (0.03–0.05 s; n=7), and 60–90 pulses per note. The dominant frequency ranges from 3.70–4.10 kHz; bandwidth values range from 1.39 (1.10–1.6) to 11.7 (11.1–13.3) kHz (n=7). Call type III can be emitted alone, after, or preceding call type I.

During periods of breeding chorus activity, males have been observed emitting a) only call type I, b) one to three type II calls, followed by a single type I call, c) emit several calls of type III followed or preceded by call type I, or d) produce all three call types sequentially (Fig. 9E). Call type I of *T. celeste* is more similar to the trills produced by *T. picta* and *T. smithii* but can be differentiated by the following characteristics (condition for *T. celeste* in parentheses): Call type I differs primarily in the number of notes per call: the trill speed is faster in *T. picta* = 60–70 notes/s and *T. smithii* = 43–51 notes/s than in *T. celeste* (25–37 notes/s; n=17). In addition, *T. picta* and *T. smithii* have a higher dominant frequency, 4.6–6.30 kHz and 4.29–6.64 kHz respectively, when compared with *T. celeste* (3.80–4.30 kHz, n = 28).



FIGURE 10. Oviposition process of *Tlalocohyla celeste* sp. nov. (A) A pair in axillary amplexus with egg deposition. (B–D) Oviposition at the end of different leaves. (E) 5 days of development. (F) 9 days of development.

Reproduction. Males of *Tlalocohyla celeste* have been observed calling year-round but display a significant increase in calling activity during periods of heightened precipitation. Vocalizations are generally first observed around 16:00 h and continue throughout the night, until sunrise. Individuals can be heard during the day, especially during periods of heavy rainfall. Most calling activity takes place along the vegetated wetland perimeter, density

of calling males decreases towards the center of the wetland where water levels are deeper. Males have been observed calling in a head-down, horizontal, or head-up position, as they perch on vegetation. Individuals occupied a variety of herbaceous plant perches, but most were found on the locally common grass *Rhynchospora corymbosa* (Cyperaceae) (Fig. 7). Calling males are positioned 0.1–3 m above the ground, either calling in isolation or in small groups, with individuals often perched as little as 15–20 cm from one another. Satellite male behavior has been observed in this species, a trait also reported for *T. picta* (Roble 1985).

Females of this species, detected less frequently than males, were observed active in the periphery of the wetland and moved around calling males. On several occasions, females were found in the interior of the forest that surrounds the wetland, some 20 m from the water's edge. Gravid females were first observed on June 12th, 2021 (Fig. 4E), followed by subsequent sightings through September.

Tlalocohyla celeste exhibits axillary amplexus (Duellman & Trueb 1986) (Fig. 4C and 10A). The first amplexant pair was discovered on June 13th, 2021 at 5:00 h. Amplexus and oviposition have been observed at night and during the pre-dawn morning hours. The amplexing pair separates immediately after oviposition.

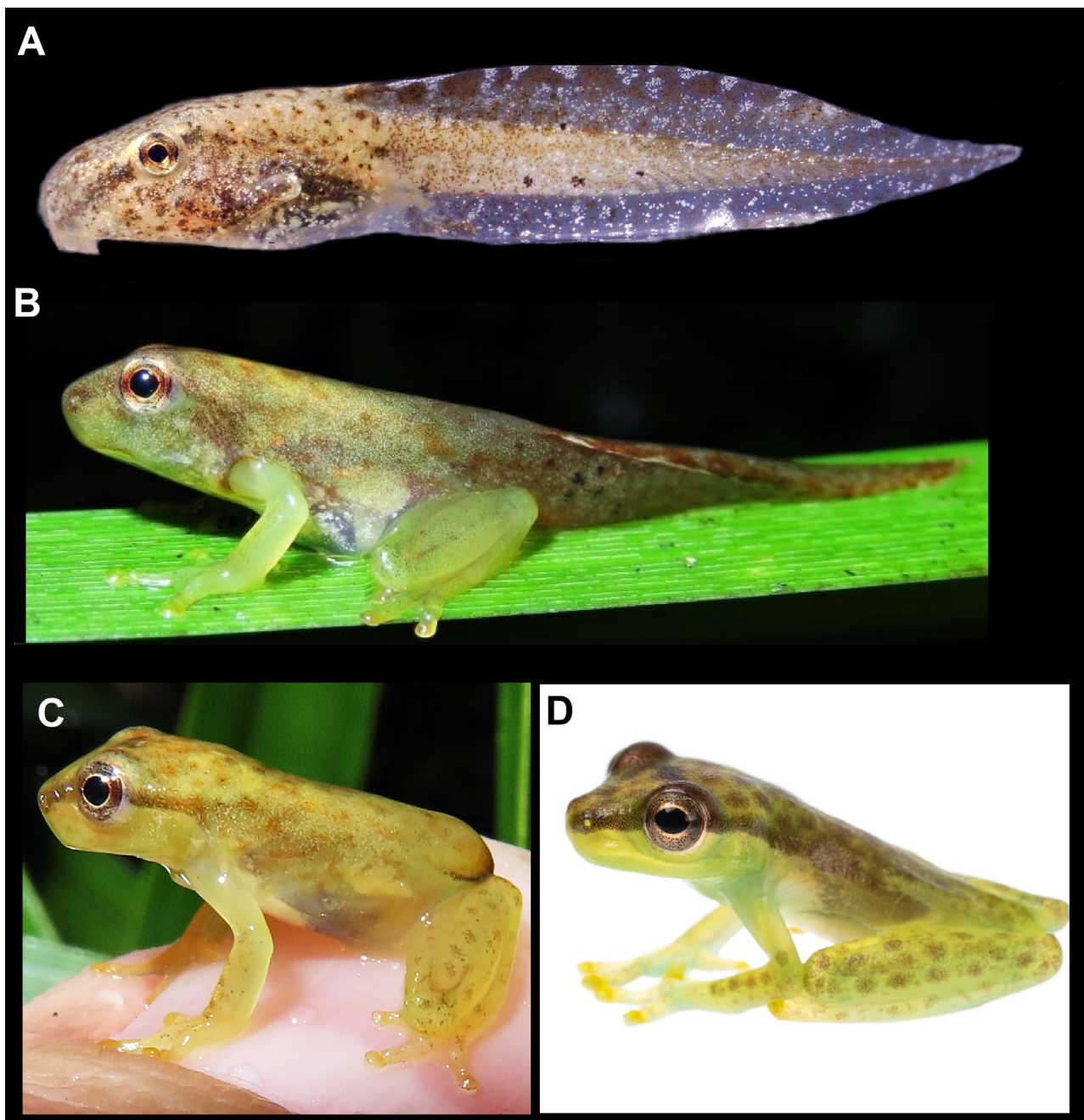


FIGURE 11. Metamorphosis of *Tlalocohyla celeste* sp. nov. (A) Tadpole at stage 35. (B) Metamorph of 11 mm of SVL. (C) Recently metamorphosed juvenile of 7 mm. (D) Juvenile.

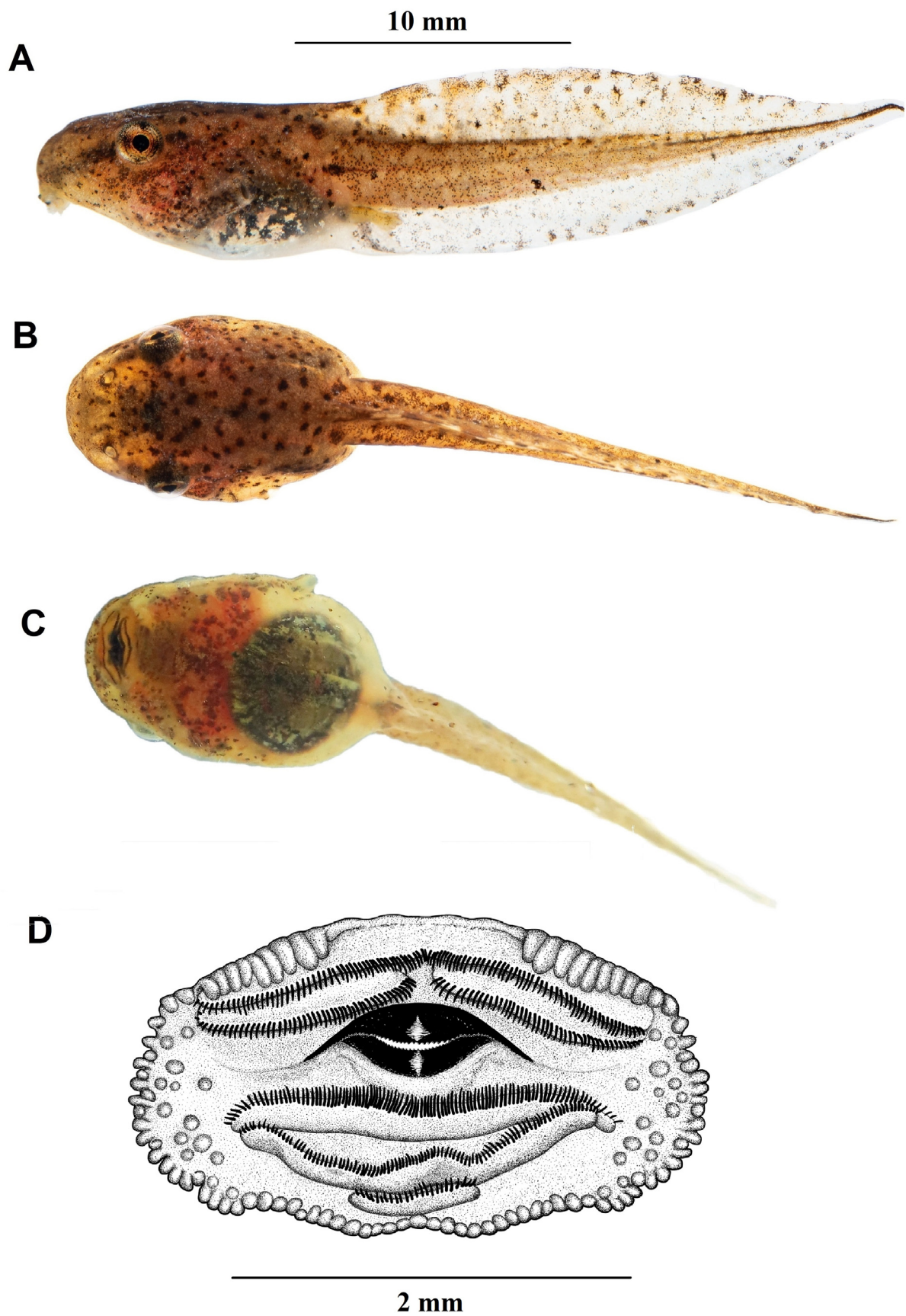


FIGURE 12. *Tlalocohyla celeste* **sp. nov.** tadpole at stage 34 (35) according to Gosner (1960). (A) Lateral view, (B) dorsal view, (C) ventral view, (D) oral disc.

All egg masses observed to date have been deposited at the tip, or along the drooping edge of leaves located directly above the water (Fig. 10). This indicates that *T. celeste* employs reproductive mode 24 (fide Haddad & Prado 2005) where arboreal eggs hatch into exotrophic tadpoles that drop into lentic water. Egg masses contain 20–61 unpigmented eggs (n=8) (Fig. 10B–D). Measurements taken from three different egg masses indicate that each clutch occupies an area between 12–22 mm in width and 23–28 mm in length; eggs measure an average of 2.0 mm in diameter (without the clear jelly capsules). One gravid female maintained in captivity for two days deposited three clutches containing 23, 45, and 61 eggs respectively, indicating that females can engage in multiple oviposition events during each breeding cycle.

Early embryos, observed five days after oviposition, were uniformly white with visible external gills (Fig. 10E). Seven days after oviposition, these embryos were light brown and marked with small black spots, particularly on the tail; the ventral region remained white. Nine days after oviposition, the embryos were brown with additional spots present on body and tail (Fig. 10F). The tadpoles hatched ten days after oviposition.

Egg masses were observed from June to November. Metamorphs and small juveniles were observed between November and June. Based on observations derived from tadpoles reared in ex-situ conditions, larval development appears to be slow. Three months after hatching, tadpoles reared under controlled conditions remained at Gosner stages 36–39 (Gosner 1960). A recent metamorph was measured to have a SVL of 7 mm (Fig. 11C).

The following anurans were observed to occur syntopically and likely share resources with *T. celeste*: *Agalychnis callidryas*, *Boana rufitela*, *Dendropsophus ebraccatus*, *Dendropsophus microcephalus*, *Dendropsophus phlebodes*, *Incilius valliceps*, *Leptodactylus melanonotus*, *Lithobates forreri*, *Lithobates vaillanti*, *Rhinella horribilis*, *Scinax boulengeri*, *Scinax elaeochroa*, *Tlalocohyla loquax*. All were confirmed to reproduce in the same wetland.

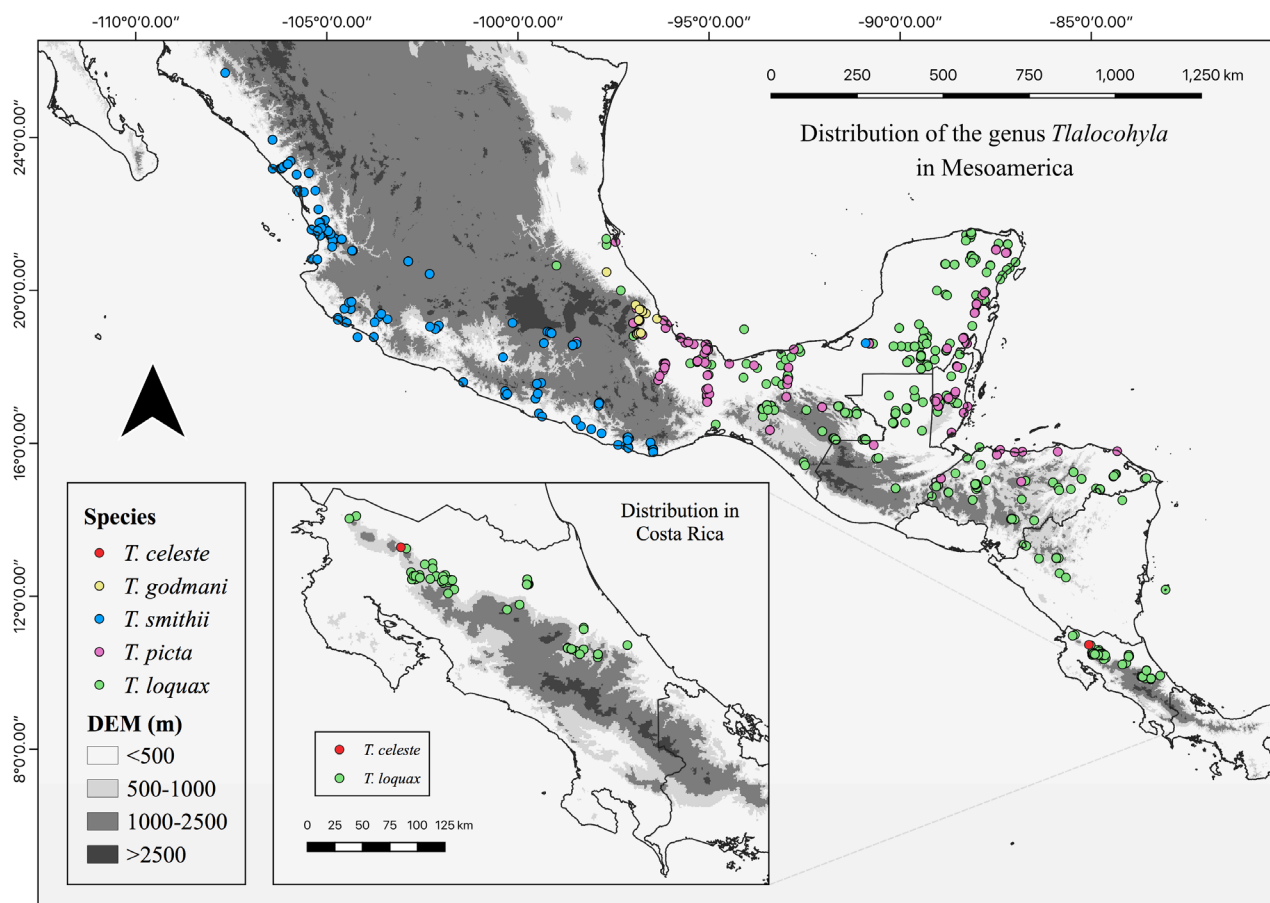


FIGURE 13. Geographic distribution of the genus *Tlalocohyla* in Mesoamerica. Inset, map of Costa Rica, showing the distribution of *Tlalocohyla loquax* (green circles) and *Tlalocohyla celeste* sp. nov. (red circle). Sources: (GBIF.org 2022).

Geographic distribution and habitat. *Tlalocohyla celeste* is only known to inhabit a single wetland system in the privately owned Tapir Valley Nature Reserve (Lat: 10.71 N Long: -85.01 W; elevation 660 m asl). The type locality is located between Tenorio and Miravalles volcanoes, in Bijagua de Upala, Alajuela Province, Costa Rica

(Fig. 13). The reserve's life zones are classified as Tropical Premontane Wet Forest and Tropical Moist Forest (Holdridge 1967). The number of dry months per year ranges from one to two, without a marked dry season. The mean annual precipitation is 3,500 mm and monthly temperatures ranges 20–33 °C (IMN 2021).

The frogs inhabit an 8-hectare marsh with a seasonally fluctuating, but permanent water level. The wetland is continually fed by a small tributary, by rainwater collected from surrounding hillsides, and likely by groundwater that wells up from bottom springs. A narrow discharge channel facilitates slow, directional water movement through the wetland. In the past, sections of this wetland have been channelized for irrigation purposes but it is now reverting to a more natural state. The surrounding hills and foothills of nearby mountains are largely forested, but areas of cultivated grassland are interspersed throughout the region. The shallow part of the marsh's littoral zone is dominated by the grass *Rhynchospora corymbosa* (Cyperaceae), whereas the riparian zone is occupied by a diverse assemblage of herbaceous vegetation (Fig. 14). Away from the water's edge, the vegetation structure changes and herbaceous plants are replaced by woody shrubs and trees, which connect to forest in the upland areas.

Tlalocohyla celeste is an abundant species within the marsh at Tapir Valley Reserve. During periods of increased activity their calls can be heard throughout the littoral zone of the wetland, and one can readily observe up to 50 individuals in a single night. Long-term monitoring is ongoing to determine the population dynamics of this species. In spite of its local abundance, repeated visual and acoustic searches in nearby wetlands within a 2 km radius that seemingly displayed similar habitat quality and characteristics have thus far not resulted in the discovery of additional *T. celeste* populations.

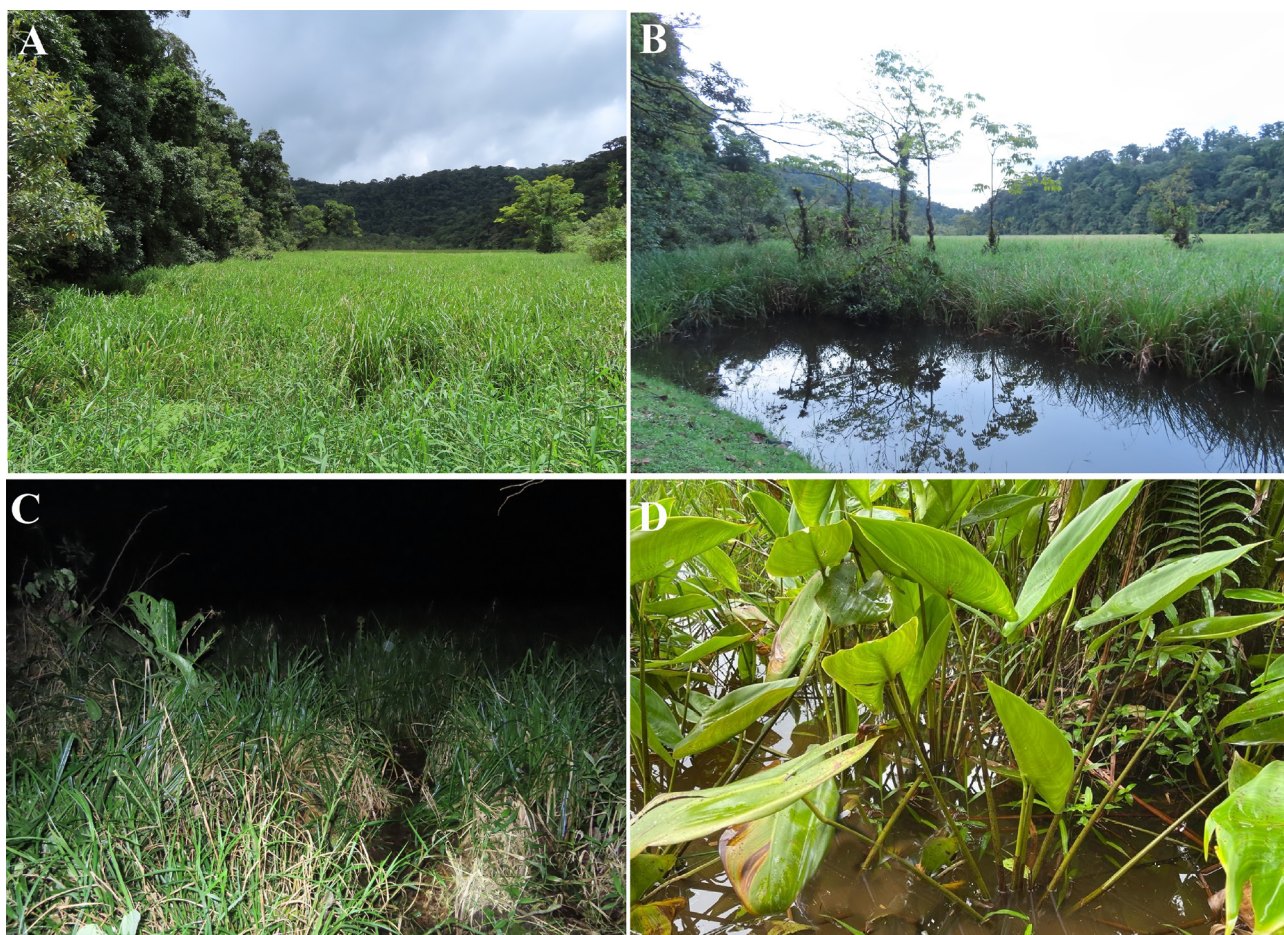


FIGURE 14. Habitat where *Tlalocohyla celeste* sp. nov. is found. General view of the north (A) and southwest (B) sector of the wetland. The habitat is dominated by the grass *Rhynchospora corymbosa* (C), but other species of plants tolerant to flooded environments can be used by the frog for its reproductive activity (D).

Natural history. Individuals of this new species have been observed catching small flies and micro moths, and presumably its diet consists of a variety of small invertebrates. Although no direct observations of predation on adult *T. celeste* were made, its wetland habitat harbors abundant snakes that are known predators of anurans. In addition, ctenid spiders, which are common frog predators, abound. During the course of our surveys, opilionid arachnids

were observed scavenging a dead frog and small wasps were seen attacking *T. celeste* egg masses and preying on early developing larvae

Etymology. The specific epithet “celeste” (light blue, or sky-blue in Spanish), is used as a noun in apposition, and refers to the striking blue coloration seen on this frog’s axillary membranes and groin area, as well as on the inflated vocal sac in adult males. Perhaps more importantly, the authors want to celebrate the river Río Celeste, famous for the distinctive turquoise-blue hue of its water, whose watershed feeds the wetlands that provide critical habitat for its namesake frog. Río Celeste represents a critical natural resource and an important economic driver for local communities, as well as a nexus for sharing the beauty of nature with visitors from outside the region. The fact that this frog was discovered through local wetland restoration efforts is a testament to the critical importance of protecting our aquatic resources.

Discussion

The decision to add this new species to the four existing species in the genus *Tlalocohyla* is adequately supported by the phylogenetic analyses. The division of the genus into the two species groups that were initially identified by Duellman (1970) is partially sustained by our Bayesian results of *T. picta* and *T. smithii* as well as by the monophyly of *T. godmani* and *T. loquax*, as proposed by Faivovich *et al.* (2018). However, the monophyly of *T. picta* and *T. smithii* has less than 50% jackknife support according to Faivovich *et al.* (2018), which was corroborated by our own ML analysis. This leaves unclear an adequate phylogenetic separation of the two groups. The only characteristics that separate the two putative species groups include: a small size, the absence or reduction of an axillary membrane, having reduced webbing on hands, and having a mating call that consists of a series of short, high-pitched notes, uniting *T. picta* and *T. smithii*, and separating these species from *T. godmani* and *T. loquax* (Duellman 1970). All of the aforementioned traits are consistent with those observed in *T. celeste*, leading us to consider that the new species would be more closely aligned with *T. picta* and *T. smithii*. The uncorrected p-distances in our analysis suggest that *T. celeste* is most closely related to *T. picta* (Table 3), but based on Bayesian inference and ML analysis, *T. celeste* appears to form a clade separate and more related to the putative *T. godmani* group. Clearly, the phylogenetic position of *T. celeste* with respect to its congeners will benefit from a more in-depth study of the phylogeny of this genus, using additional markers and more specimens from each of the five species of *Tlalocohyla*.

TABLE 3. Uncorrected p-distances between the 16S fragment among specimens of *Tlalocohyla*, expressed as percentage.

	1	2	3	4	5	6
<i>Tlalocohyla celeste</i> ECB-Anf-f50-08-0101	-					
<i>Tlalocohyla celeste</i> YPM_13222	0.00	-				
<i>Tlalocohyla godmani</i> DQ830811.1	10.801	10.801	-			
<i>Tlalocohyla loquax</i> DQ055822.1	9.948	9.948	9.773	-		
<i>Tlalocohyla picta</i> AY843654.1	9.408	9.408	11.498	10.122	-	
<i>Tlalocohyla picta</i> DQ830812.1	9.408	9.408	11.498	10.122	0.00	-
<i>Tlalocohyla smithii</i> DQ830812.1	11.344	11.344	11.693	12.587	11.344	11.344

From the larval perspective, Faivovich *et al.* (2005) mentioned that the larvae of *T. loquax* and *T. smithii* share a reduction in the length of the third posterior tooth row, a condition shared with *T. celeste* but not with *T. godmani* or *T. picta*. The larval character of having a significantly reduced posterior third row of teeth and having the dorsal fin originating near the base of the tail is shared between *T. celeste* and *T. smithii*.

To date, *Tlalocohyla* has no suggested putative morphological synapomorphy (Faivovich *et al.* 2005; 2018) and our topologies also do not help suggesting any. Character states shared between *T. celeste*, *T. picta* and *T. smithii* optimize either as originating in the ancestor of *Tlalocohyla* and later lost in the *T. godmani* group or as two independent gains in *T. celeste* and the *T. picta* group. Additionally, we recover *Isthmohyla* paraphyletic in respect

to *Tlalocohyla*. However, the question on the paraphyly of *Isthmohyla* has been thoroughly discussed in Faivovich et al. (2018) and our analyses, using fewer markers, were not designed to test relationships between Hyline clades; only to suggest a generic allocation of our species.

Literature on oviposition sites utilized by other *Tlalocohyla* species indicates that *T. picta* and *T. loquax* deposit their eggs directly in the water, generally attached to aquatic vegetation (Duellman 1970, 2001, Lee 1996, Lee 2000, Savage 2002). No specific information on oviposition site selection in *T. smithii* or *T. godmani* could be found. The fact that *T. celeste* egg clutches were invariably found out of the water, attached to emergent vegetation, suggests that this species deploys a different reproductive mode than other *Tlalocohyla* species. Elucidating the reproductive modes of *T. smithii* and *T. godmani* will help provide perspective on whether its specific breeding mode adds another character trait that diverges *T. celeste* from its presumed closest relatives.

On a landscape ecology-level, the occurrence of this new species at Tapir Valley Nature Reserve is equally surprising. The Guanacaste mountain range (Cordillera de Guanacaste) constitutes the continental divide in northern Costa Rica; it provides a physical barrier between the Caribbean and Pacific slopes and their respective, very different climate regimes. Although located in very close proximity to the continental divide, the type locality is situated on the Caribbean-facing slope of Tenorio Volcano and therefore not subject to the prolonged, seasonally arid conditions that exist on the Pacific-facing slopes and valleys of the same mountain.

As mentioned previously, *T. celeste* is only known from a single 8-hectare wetland. More than ten months of targeted visual and acoustic surveys in nearby wetlands have not resulted in the discovery of additional populations. At this time, *T. celeste* appears to be isolated to this one wetland system, and this unique population could be in danger due climate change and vegetative succession. While the population appears robust, we suggest that further population studies are necessary to determine the true conservation status of this species.

The wetland system that is home to *T. celeste* harbors an amphibian species assemblage that is typical for vegetated lentic and lotic wetlands in the region. All other co-occurring anuran species are adaptable and common in the region. Likewise, the vegetation assembly associated with the benthic, riparian, and upland ecotones appear similarly unsurprising. It is noteworthy that this wetland has only been in its current state for a relatively short period. The property was acquired in the early 2000s, at which point it was still intensively grazed pasture land. Only a small portion of the current marsh was in existence then, severely impacted by the cattle that used it as a watering hole. Converting the land from cattle farming, changes to its hydrology, and ongoing environmental restoration efforts have resulted in the wetland system that exists today, a mere 17 years after the land was protected. Tapir Valley Nature Reserve's history of human impact, long-term habitat degradation, and, recently, the restoration of the site's habitats speaks to an assumption that the species inhabiting this system, including *T. celeste*, display a significant degree of adaptability and resilience. This assumption is further strengthened by the notion that *T. picta* and *T. smithii* are known to inhabit and breed in temporarily flooded and permanent wetlands during the rainy season, and both have been found in nearby forested areas outside periods of reproductive activity. Both species reportedly adapt well to anthropogenic landscapes and are regularly found in close proximity to human settlements (e.g. Campbell 1998, Lee 1996, Leenders 2016, Lemos-Espinal & Dixon 2013, Luna-Gómez *et al.* 2017, McCranie & Wilson 2002).

It is our hope that *T. celeste* turns out to be as adaptable and resilient as its close relatives and may eventually be found in additional sites in the region. Zumbado-Ulate *et al.* (2021), after evaluating the conservation status of Costa Rican tree frog species, postulate that tree frogs are a particularly informative group to evaluate the persistence and resilience of populations. They also suggest that designation of an iconic frog as a flagship species to raise awareness for the conservation of amphibians could prove to be a worthwhile strategy to pursue. For the time being, we rejoice in the fact that community awareness and bold conservation actions by a few individuals have resulted in the protection and restoration of a valuable aquatic resource and its surrounding habitats, which now provide a home for a thriving population of the endangered Baird's Tapir (*Tapirus bairdii*), and numerous birds, fish, reptiles, and amphibians, rather than just cattle. The discovery of *T. celeste* in this active restoration site will undoubtedly empower the community to continue their conservation efforts and provide further incentive to unite landowners and area conservation partners into collaborative research and implementation efforts that could serve as an exciting model for other regions.

Acknowledgements

We want to thank the Ministry of Environment and Energy of the Republic of Costa Rica (MINAE), National System of Conservation Areas (SINAC), especially the rangers of Area de Conservacion Arenal Tempisque (ACAT), for help with permissions for the activities described in this document (M-P-SINAC-PNI-ACAT-043-2021), and the National Commission for Biodiversity Management (CONAGEBIO) for facilitate the genetic component of this project (R-006-2022-OT-CONAGEBIO). We are grateful to Tapir Valley Nature Reserve for providing access to the field sites and logistical support. Andy Whitworth was the first herpetologist to actually pay attention to Donald and connected him with Twan Leenders and his team. We thank Re:Wild Foundation and Costa Rica Wildlife Foundation, especially the staff of Costa Rica Wildlife Foundation: Sofia Pastor Parajeles, Sara Garcia, Galdric Mossol, Neus Mairal and Elena Baeta for providing valuable assistance in the field during the expeditions. We thank Gabriela Hernández Mora from the Bacteriology Laboratory of the National Animal Health Service (SENASA) who graciously facilitated the use of laboratory equipment. We are especially grateful to Josimar Estrella Morales and other researchers from the molecular department of the SENASA Biosecurity Laboratory for assistance with DNA extraction and sequencing. We also thank Lilliana Piedra Castro from the Natural Resources and Wildlife Laboratory (LARNAVISI) for her support and institutional backing, as well as Rodolfo Umaña Castro and Carolina Sancho Blanco from the Genomic Analysis Laboratory (LAGEN) for their support in the use of laboratory facilities, Mauricio Herrera Campos from the Zoology Museum of the National University, Gerardo Chávez from the Zoology Museum of the University of Costa Rica and Rolando Ramirez Campos for help in finding equipment. We thank Armando Estrada Chavarría and Francisco Durán Alvarado from the Department of Natural History of the National Museum, who helped with the identification of *Rhynchospira corymbosa*.

References

- Altig, R. & McDiarmid, R.W. (1999) Body plan: development and morphology. In: McDiarmid, R.W. & Altig, R. (Eds.), *Tadpoles: The Biology of Anuran Larvae*. University of Chicago Press, Chicago, Illinois, pp. 24–51.
- AmphibiaWeb (2022) AmphibiaWeb: Information on Amphibian Biology and Conservation. Available from: <https://amphibiaweb.org/> (accessed 1 January 2022)
- Araujo-Vieira, K., Tacioli, A., Faivovich, J., Orrico, V.G.D. & Grant, T. (2015) The tadpole of *Sphaenorhynchus caramaschii*, with comments on larval morphology of *Sphaenorhynchus* (Anura: Hylidae). *Zootaxa*, 3904 (2), 270–282. <https://doi.org/10.11646/zootaxa.3904.2.6>
- Boulenger, G.A. (1902) [1901] Reptilia and Batrachia. *Zoological Record*, 38, 1–35.
- Caldwell, J.P. (1986) A description of the tadpole of *Hyla smithii* with comments on tail coloration. *Copeia*, 1986 (4), 1004–1006.
- Campbell, J.A. (1998) *Amphibians and Reptiles of northern Guatemala, the Yucatán, and Belize*. University of Oklahoma Press, Norman, Oklahoma, 380 pp.
- Cisneros-Heredia, D.F. & McDiarmid, R.W. (2007) Revision of the characters of Centrolenidae (Amphibia: Anura: Athesphatanura), with comments on its taxonomy and the description of new taxa of glass frogs. *Zootaxa*, 1572 (1), 1–82. <https://doi.org/10.11646/zootaxa.1572.1.1>
- Duellman, W.E. (1970) *The Hylid Frogs of Middle America*. Museum of Natural History, The University of Kansas, Lawrence, Kansas, 753 pp.
- Duellman, W.E. (2001) *The Hylid Frogs of Middle America*. Society for the Study of Amphibians and Reptiles, Lawrence, Kansas, 1158 pp.
- Duellman, W.E. & Trueb, L. (1986) *Biology of Amphibians*. The Johns Hopkins University Press, Baltimore, Maryland and Ithaca, New York, 670 pp.
- Faivovich, J. (2002) A cladistic analysis of *Scinax* (Anura: Hylidae). *Cladistics*, 18 (4), 367–393. <https://doi.org/10.1111/j.1096-0031.2002.tb00157.x>
- Faivovich, J., Haddad, C.F.B., García, P.C.A., Frost, D.R., Campbell, J.A. & Wheeler, W.C. (2005) Systematic review of the frog family Hylidae, with special reference to Hyalinae: phylogenetic analysis and taxonomic revision. *Bulletin of the American Museum of Natural History*, 294, 1–240. [https://doi.org/10.1206/0003-0090\(2005\)294\[0001:SR0TFF\]2.0.CO;2](https://doi.org/10.1206/0003-0090(2005)294[0001:SR0TFF]2.0.CO;2)
- Faivovich, J., Pereyra, M.O., Luna, M.C., Hertz, A., Blotto, B.L., Vásquez-Almazán, C.R., McCranie, J.R., Sánchez, D.A., Baêta, D., Araujo-Vieira, K., Köhler, G., Kubicki, B., Campbell, J.A., Frost, D.R., Wheeler, W.C. & Haddad, C.F.B. (2018) On the monophyly and relationships of several genera of Hylini (Anura: Hylidae: Hyalinae), with comments on recent taxonomic changes in hylids. *South American Journal of Herpetology*, 13 (1), 1–32. <https://doi.org/10.2994/SAJH-D-17-00115.1>

- Frost, D.R. (2022) Amphibian Species of the World: An Online Reference. Version 6.1. Available from: <https://amphibiansoftheworld.amnh.org/> (accessed 18 April 2022)
- Gaige, H.T. & Stuart, L.C. (1934) A new *Hyla* from Guatemala. *Occasional Papers of the Museum of Zoology*, 281, 1–3.
- GBIF (2022) GBIF Occurrences Download. *T. picta*. *T. smithii*. *T. loquax*. *T. godmani*. Available from: <https://doi.org/10.15468/dl.q526bn>, <https://doi.org/10.15468/dl.bjy9uf>, <https://doi.org/10.15468/dl.65qqe9>, <https://doi.org/10.15468/dl.qdcq7h> (accessed 11 January 2022)
- Gosner, K.L. (1960) A simplified table for staging anuran embryos and larvae with notes on identification. *Herpetologica*, 16 (3), 183–190.
- Grosjean, S. (2005) The choice of external morphological characters and developmental stages for tadpole-based anuran taxonomy, a case study in *Rana (Sylvirana) nigrovittata* (Blyth, 1855) (Amphibia, Anura, Ranidae). *Contributions to Zoology*, 74 (1–2), 61–76.
<https://doi.org/10.1163/18759866-0740102005>
- Günther, A.C.L.G. (1901) Reptilia and Batrachia. In: Salvin, O. & Godman, F.D. (Eds.), *Biologia Centrali Americana*. R.H. Porter & Dulau & Co, London, pp. 269–292.
- Haddad, C.F.B. & Prado, C.P.A. (2005) Reproductive modes in frogs and their unexpected diversity in the Atlantic Forest of Brazil. *BioScience*, 55 (3), 207–217.
[https://doi.org/10.1641/0006-3568\(2005\)055\[0207:RMIFAT\]2.0.CO;2](https://doi.org/10.1641/0006-3568(2005)055[0207:RMIFAT]2.0.CO;2)
- Heyer, W.R., Rand, A.S., Cruz, C.A.G., Peixoto, O.L. & Nelson, C.E. (1990) Frogs of Boracéia. *Arquivos de Zoologia*, 31 (4), 231–410.
- Holdridge, L.R. (1967) *Life Zone Ecology*. Tropical Science Center, San José, 206 pp.
- Huelsenbeck, J.P. & Ronquist, F. (2001) MRBAYES: Bayesian inference of phylogenetic trees. *Bioinformatics*, 17 (8), 754–755.
<https://doi.org/10.1093/bioinformatics/17.8.754>
- IMN [Instituto Meteorológico Nacional] (2021) Mapas de Costa Rica, Datos Climáticos, Upala Período: 1998–2018. Available from <https://www.imn.ac.cr/mapa> (accessed 23 November 2021)
- IUCN (2012) *Categorías y Criterios de la lista roja de la UICN. Versión 3.1. Segunda Edición*. IUCN, Gland, Cambridge, 34 pp.
- Köhler, G. (2011) *Amphibians of Central America*. Herpeton Verlag, Offenbach, 379 pp.
- Köhler, G. (2012) *Color Catalogue for Field Biologists*. Herpeton Verlag, Offenbach, 49 pp.
- Kok, P.J.R. & Kalamandeen, M. (2008) *Introduction to the taxonomy of the amphibians of Kaieteur National Park, Guyana*. Belgian Development Corporation, Brussels, 278 pp.
- Lavilla, E.O. & Scrocchi, G.J. (1986) Morfometría larval de los géneros de Telmatobiinae (Anura, Leptodactylidae) de Argentina y Chile. *Physis*, 44 (106), 39–43.
- Lee, J.C. (1996) *The Amphibians and Reptiles of the Yucatan Peninsula*. Cornell University Press, Ithaca, New York, 500 pp.
- Lee, J.C. (2000) *A field guide to the amphibians and reptiles of the Maya world: the lowlands of Mexico, northern Guatemala, and Belize*. Cornell University Press, Ithaca, New York, 402 pp.
- Leenders, T. (2016) *Amphibians of Costa Rica, a field guide*. Cornell University Press, Ithaca, New York, 531 pp.
- Lemos-Espinal, J.A. & Dixon, J.R. (2013) *Amphibians and Reptiles of San Luis Potosí*. Eagle Mountain Publishing, LLC, Eagle Mountain, Utah, 300 pp.
- Luna, M.A., McDiarmid, R.W. & Faivovich, J. (2018) From erotic excrescences to pheromone shots: structure and diversity of nuptial pads in anurans. *Biological Journal of the Linnean Society*, 124 (3), 1–44.
- Luna-Gómez, M.I., García, A. & Santos-Barrera, G. (2017) Spatial and temporal distribution and microhabitat use of aquatic breeding amphibians (Anura) in a seasonally dry tropical forest in Chamela, Mexico. *Revista de Biología Tropical*, 65 (3), 1082–1094.
- Lynch, J.D. & Duellman, W.E. (1997) Frogs of the genus *Eleutherodactylus* (Leptodactylidae) in western Ecuador: systematics, ecology, and biogeography. *The University of Kansas Natural History Museum Special Publications*, 23, 1–236.
- McCranie, J.R. & Wilson, L.D. (2002) *The Amphibians of Honduras*. Society for the Study of Amphibians and Reptiles, Ithaca, New York, 667 pp.
- Myers, C.W. & Duellman, W.E. (1982) A new species of *Hyla* from Cerro Colorado, and other tree frog records and geographical notes from Western Panama. *American Museum Novitates*, 1982 (2752), 1–32.
- Novaes-E-Fagundes, G., Araujo-Vieira, K., Entiauspe-Neto, O.M., Roberto, I.J., Orrico, V.G.D., Solé, M., Haddad, C.F.B. & Loebmann, D. (2021) A new species of *Scinax* Wagler (Hylidae: Scinaxini) from the tropical forests of Northeastern Brazil. *Zootaxa*, 4903 (1), 1–41.
<https://doi.org/10.11646/zootaxa.4903.1.1>
- Rambaut, A. (2014) FigTree. Version 1.4.2. A graphical viewer of phylogenetic trees. Available from <http://tree.bio.ed.ac.uk/software/figtree/> (accessed 11 January 2022)
- Roble, S.M. (1985) Observations on Satellite Males in *Hyla chrysoscelis*, *Hyla picta*, and *Pseudacris triseriata*. *Journal of Herpetology*, 19 (3), 432–436.
- Ronquist, F. & Huelsenbeck, J.P. (2003) Mrbayes 3: Bayesian phylogenetic inference under mixed models, *Bioinformatics*, 19 (12), 1572–1574. <https://doi.org/10.1093/bioinformatics/btg180>
- Savage J.M. (2002) *The amphibians and reptiles of Costa Rica. A herpetofauna between two continents, between two seas*. The

University of Chicago Press, Chicago, Illinois, 954 pp.

- Savage, J.M. & Heyer, W.R. (1967) Variation and distribution in the tree-frog genus *Phyllomedusa* in Costa Rica, Central America. *Studies on Neotropical Fauna and Environment*, 5 (2), 111–131.
<https://doi.org/10.1080/01650526709360400>
- Sela, I., Ashkenazy, H., Katoh, K. & Pupko, T. (2015) GUIDANCE2: accurate detection of unreliable alignment regions accounting for the uncertainty of multiple parameters. *Nucleic Acids Research*, 43 (1), 7–14.
<https://doi.org/10.1093/nar/gkv318>
- Taboada, C., Brunetti, A.E., Lyra, M.L., Fitak, R.R., Faigon, S.A., Ron, S.R., Lagorio, M.G., Haddad, C.F.B., Lopes, N.P., Johnsen, S., Faivovich, J., Chemes, L.B. & Bari, S.E. (2020) Multiple origins of green coloration in frogs mediated by a novel biliverdin-binding serpin. *Proceedings of the National Academy of Sciences of the United States of America*, 117 (31), 18574–18581.
- Tamura, K., Peterson, D., Peterson, N., Stecher, G., Nei, M. & Kumar, S. (2011) MEGA5: molecular evolutionary genetics analysis using maximum likelihood, evolutionary distance, and maximum parsimony methods. *Molecular Biology and Evolution*, 28 (10), 2731–2739.
<https://doi.org/10.1093/molbev/msr121>
- Thompson, J.D., Higgins, D.G. & Gibson, T.J. (1994) CLUSTAL W: improving the sensitivity of progressive multiple sequence alignment through sequence weighting, position-specific gap penalties and weight matrix choice. *Nucleic Acids Research*, 22 (22), 4673–4680.
<https://doi.org/10.1093/nar/22.22.4673>
- Watters, J.L., Cummings, S.T., Flanagan, R.L. & Siler, C.D. (2016) Review of morphometric measurements used in anuran species descriptions and recommendations for a standardized approach. *Zootaxa*, 4072 (4), 477–495.
<http://doi.org/10.11646/zootaxa.4072.4.6>
- Zumbado-Ulate, H., Searle, C.L., Chaves, G., Acosta-Chaves, V., Shepack, A., Salazar, S. & García-Rodríguez, A. (2021) Assessing Suitable Habitats for Treefrog Species after Previous Declines in Costa Rica. *Diversity*, 13 (11), 577.
<https://doi.org/10.3390/d13110577>

SUPPORTING INFORMATION

SUPPLEMENTARY MATERIAL 1. Nexus file of the alignment of the new species and 141 sequences provided by Faivovich *et al.* (2018).

See download link on the DOI landing page

SUPPLEMENTARY MATERIAL 4. Sequences of 12s from the genus *Tlalocohyla* with gen bank accession numbers.

See download link on the DOI landing page

SUPPLEMENTARY MATERIAL 5. Sequences of 16s from the genus *Tlalocohyla* with gen bank accession numbers.

See download link on the DOI landing page